Dinoop Lal S. “Photodegradation of polystyrene by nano titanium dioxide and photosensitizers.” Thesis. Research & Postgraduate Department of Chemistry, St. Thomas’ College (Autonomous), Thrissur, University of Calicut, 2020.

Chapter 1

Introduction and Review of Literature

1.1 A glimpse into the polymer history

Human beings have been enjoying the benefits of polymer materials since 1600 BC when Mesoamericans processed natural rubber for their specific uses. They moulded several materials ranging from bands to sculptures using natural rubber[1]. Human beings have been experimenting on various natural resources for developing rubbers, resins and waxes for their uses. 19th century witnessed some advances in the polymer chemistry with the invention of vulcanized rubber in 1839 AD by Charles Goodyear by heating natural rubber with sulphur at 132°C[2]. Polystyrene was discovered by Eduard Simon in the same year. In 1907, a Belgian-American chemist named Leo Baekeland condensed phenol with formaldehyde and developed phenol formaldehyde resin most commonly called bakelite. It is hard and used as insulators in electrical appliances even today especially in switch boards. The new era of polymer technology began in 1922 when an Austrian-American Chemist Herman Francis Mark proved that polymers are made up of macromolecules instead of aggregations of small molecules. This was very much in support to the ideas of the German Chemist Hermann Staudinger. Staudinger published a paper in 1920 titled as "Über Polymerisation" based on the modern polymer theories[3]. During the 19th century many classes of polymers were synthesized and developed which found applications in various sectors replacing wood, metals, stones, bones, glasses etc. Polymers including polystyrene (PS), polycarbonates (PC), polyvinyl chloride (PVC), polypropylene (PP), polyphenylene oxide (PO), polyesters (PES), acrylonitrile-butadiene-styrene copolymer (ABS), polyurethane (PU) etc., were commercialized during the 19th and 20th centuries[4]. Polymers were classified as natural, synthetic and semi-synthetic based upon their origin. Development of new types of polymers further widened their classification based on their structures (linear, branched and cross-linked), mode of polymerization (addition and condensation polymers), molecular forces as (elastomers, thermosetting plastics, thermoplastics and fibers) and so on. Polymers with the property of plasticity were in good demand. Such polymers began

to be known as "plastics" in general. Plasticizers were developed which enhanced the properties of some rigid plastics. The so called plastics exhibited superior properties compared to other materials where ever it was applied.

The past few decades witnessed a steep rise in the amount of plastics consumed by the humanity. The global plastic production which was estimated to be around 2 metric tons in 1950 increased to 7300 metric tons in 2015. 92% of the plastics ever made include PE, PP, PVC, PS, PET, PU etc. These plastics are very much in demand for construction works, packing and so on[5]. The demand of polymer plastics are still increasing in such a way that we are unable to think of a world without them.

1.2 Polystyrene (PS)

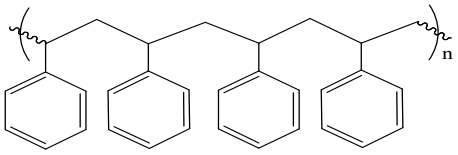

Polystyrene

Polystyrene (PS) could be considered one of the most widely used polymer material meeting the needs of human society in the form of various commodities[6,7]. Styrene monomer units polymerise to form a colourless thermoplastic resin - PS whose tacticity depends upon the mechanism adopted or catalyst used in the polymerisation process. The wide use of PS in industries, constructions, packing, automobiles and common house hold goods began when PS was commercialised in 1930s after its accidental discovery by Eduard Simon (German apothecary) in 1839. In order for PS to be useful commercially, its weight average molecular weight ($\bar{M}_w$) should be ten times its chain entanglement molecular weight ($\bar{M}_e$). Like most other polymers, the mechanical properties (tensile, flexural, impact etc.) of PS depends very much on $\bar{M}_w$. PS having $\bar{M}_w$ lesser than $\bar{M}_e$ has not much industrial significance as it remains just in white powdery form that cannot be moulded into desired commodities or useful parts owing to its week mechanical properties. The $\bar{M}_e$ of PS is ~18100 and hence PS with $\bar{M}_w$ lesser than this value is not used [8,9].

1.2.1. Tacticity in PS and its significance

The orientation of phenyl rings in PS chain determines its tacticity. If the phenyl rings are arranged in the same side of the chain we have *isotactic* PS (Figure 1.1).

Alternate arrangement of phenyl groups result in *syndiotactic* PS. Random arrangement of phenyl groups give *atactic* PS.

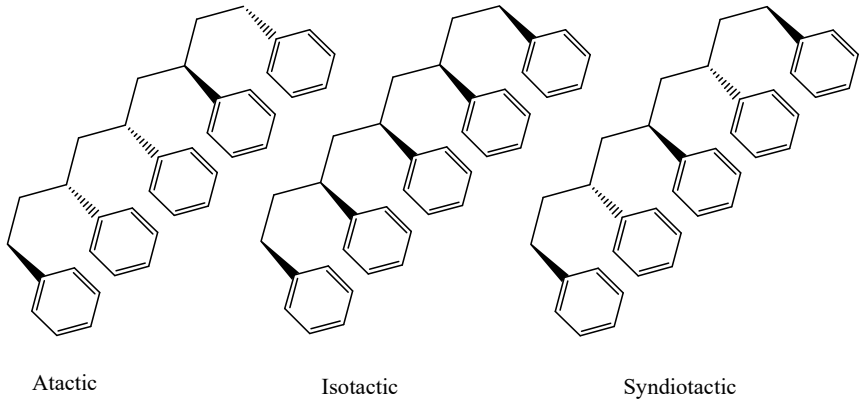

Figure 1.1. *Illustration of tacticity in PS*

The commercially produced *general purpose polystyrenes (GPPS)* are atactic. They are amorphous in nature and hard. Free-radical polymerisation results in atactic PS. The glass transition temperature (T_g) of atactic PS is around 100°C. Isotatic PS is not produced commercially. They are more crystalline compared to atactic PS. They are prepared by coordination polymerisation (Ziegler-Natta type) using stereospecific catalysts such as $TiCl_3$ activated by triethylaluminium. They melt at a temperature around 240°C[10]. Even though the catalyst used for the preparation of isotactic PS was reported in 1986[11], they are not produced due to their commercial insignificance. The reason for this is their slow crystallisation and difficulty in preparation (compared to atactic PS and syndiotactic PS). Syndiotactic PS is also crystalline with Tg around 270°C[10]. The method of preparation of sydiotactic PS also involves polymerisation using Ziegler-Natta type catalysts. Soluble complexes of titanium combined with alkyl aluminium (say $(\eta^5\text{-}C_5H_5)TiCl_3$ with methylaluminoxane $(Al(CH_3)_xO_y)_n$) gives syndiotactic PS. Crystallisation of syndiotactic PS is relatively fast. This type of PS is also not produced commercially (however some industries produce syndiotactic PS for special purposes).

Soon after the discovery of isotactic PS by Natta (1955), studies regarding the stereospecific process of PS preparation was put into practice[12]. Several authors have reported articles related to the determination of tacticity of PS through various techniques. NMR spectroscopy was an important tool used to determine the tacticity of PS during those days. The NMR proton chemical shifts could be accessed in order

to determine the tacticity of the PS chain. Even though separate peaks corresponding to α-proton of isotactic PS have been identified, attempts to resolve this peak from that of other protons of the polymer remained almost impossible. In 1962, Brownstein et al. resolved the α-proton of PS by deuteriating the β- protons and hence nullifying the spin-spin coupling of the chain by which isotactic, syndiotactic as well as heterotactic PS could be distinguished[13]. In order to minimise the solvent effect Brownstein and co-workers used benzene as solvent. Benzene solvent unlike other solvents maximised the chemical shift of α-protons. Separate peaks corresponding to α-protons of isotactic, syndiotactic and heterotactic PS were identified. Bovey et al. (1965) reported that the ^{1}H NMR signal of methylene proton of atactic PS appeared as a broad resonance[14]. Heatly and Bovey (1968) showed that the ^{1}H NMR signal of methylene proton of isotactic PS appeared as distinguishable non equivalent peaks[15]. Matsuzaki et al. (1974) reported that signals of methyl protons showed a chemical shift in the order isotactic>atactic>syndiotactic PS towards higher magnetic field in their ^{1}H NMR spectra [16]. In 1986, Ishihara and co-workers studied the stereoregularity in syndiotactic PS through XRD, ^{1}H NMR, ^{13}C NMR and IR spectroscopy[11]. The ^{1}H NMR and ^{13}C NMR spectra made it easy to distinguish between the PS of different tacticity just by observing the chemical shifts and splitting patterns of the peaks. IR spectra of syndiotactic PS as reported by Ishihara et al showed the absence of helical conformation of PS chain, as reported earlier in the case of isotactic PS by Tadokoro et al. (1961)[17]. Even though several authors have studied the NMR spectra of PS [18–21] the assignment of methylene carbon of PS backbone faced a big divergence in opinion until in 1996 Cheng and Lee deconvoluted the broad overlapped resonance of methylene carbon assisted by computer analysis[22]. With the development of various analytical tools the characterisation of tacticity of PS became much easier. Lots of articles were published on this topic recently and many works are in progress.

Tacticity of PS has a lot to tell about the physical and chemical properties of PS. Researchers worldwide have studied the dependence of tacticity of PS in its chemical and physical properties. Several authors including Tan et al. (1983)[23], Clark et al (1983)[24], Gan et al. (1985) [25] and Gan et al. (1986)[26] studied the gelation property of atactic PS. Even though polymers that have appreciable crystallinity or stereo regular sequence are the only ones that are supposed to exhibit gelation, the contrary has taken place in the case of amorphous PS (by showing gelation property). The problem

was solved in 1987 by Jeanne François and co-workers who studied the phenomenon of gelation of atactic as well as isotactic PS in CS_2 and reported that gelation observed in the solution of amorphous atactic PS was due to the presence of certain amount of syndiotactic sequence in it[27]. David et al. (1973) reported that the fluorescence yield increased with crystallinity of PS at room temperature. The excimer fluorescence followed the order isotactic crystallised>isotactic amorphous>atactic oriented>atactic amorphous[28]. Chen et al. (2003) compared the thermal stability of atactic, syndiotactic and isotactic PS and concluded that isotactic PS exhibited far better thermal stability compared to the other two. Higher activation energy required to degrade isotactic PS, supported by restricted molecular mobility explained this observation[29]. The viscoelastic property of isotactic PS was found to be lower than that of atactic and syndiotactic PS by one order of magnitude. This was due to the difference in entanglement molecular weight ($\bar{M}_e$) at a fixed weight average molecular weight ($\bar{M}_w$) as reported by Huange et al. (2011)[30]. Grigoriadi et al. (2019) studied the ageing kinetics of PS using flash-differential scanning calorimetry. He reported that the ageing kinetics followed the order isotactic PS>atactic PS>syndiotactic PS[31].

1.2.2. Polymerisation techniques for PS production

PS is prepared through addition polymerisation. The different kinds of addition polymerisation techniques that could be employed are (i) anionic (ii) cationic (iii) free-radical and (iv) coordination (Ziegler-Natta) polymerisation[9,32].

(i) **Anionic polymerisation**: Sequential steps of initiation, propagation and termination take place. The polymer formed have polydispersity index (PDI) less than 1.1 [PDI= weight average molecular weight ($\bar{M}_w$)/number average molecular weight ($\bar{M}_n$)]. One of the advantages of this method is that the structure of end-groups could be controlled by controlling the chain termination step. The disadvantage is that the polymerisation feed needs purification which determines the purity of the polymer product.

(ii) **Cationic polymerisation**: This process is generally not employed due to the difficulty in the production of high molecular weight PS. The cation intermediate (polystyrylcarbocation) is not much stable and results in fast termination of the

polymerisation process leading to low molecular weight PS. In addition to this the polymerisation feed needs purification.

(iii) **Free-radical polymerisation**: The process takes place through simultaneous initiation, propagation and termination steps. The polymer formed will have a PDI greater than 2. Variety of end products is formed in this process due to multiple termination steps. These facts confirm that free-radical polymerisation is not as organised as anionic polymerisation. The advantage of free-radical polymerisation is that the polymerisation feed requires no purification.

(iv) **Coordination polymerisation (Ziegler-Natta polymerisation):** This type of polymerisation is generally employed where polymer of high crystallinity is in demand. Catalysts are introduced in this process. The polymerisation takes place on the surface of the catalysts used. The resulting polymer product formed will have higher melting temperatures compared to their amorphous counter parts. Ziegler-Natta polymerisation is not employed in the production of cheap PS for daily usages. The polymer formed through this method will have a PDI ≈2.

Out of the above mentioned methods, the most widely used one by the industries for the production of commercial polystyrene is free-radical polymerisation. The process needs less effort as the monomer need not be cleaned during the process as mentioned above. Since the initiator residues left behind has less impact on the properties of PS formed, they (initiator) need not be removed[33]. The mechanism of free-radical polymerisation of PS formation was studied by Florey (1937)[34]. According to Florey, PS is formed when molecules of styrene are involved in a bond forming reaction through 1, 4-diradical formation as illustrated in Figure 1.2.1. Later in 1968, Mayo proposed another mechanism in which he describes the formation of a dimer through the Diels-Alder reaction involving two styrene monomers followed by the reaction between dimer and styrene to form PS (Figure 1.2.2)[35]. Later in 1988, Mulzer and co-workers proposed a mechanism where the diradical suggested by Florey could lead to the dimer suggested by Mayo (Figure 1.2.3)[36].

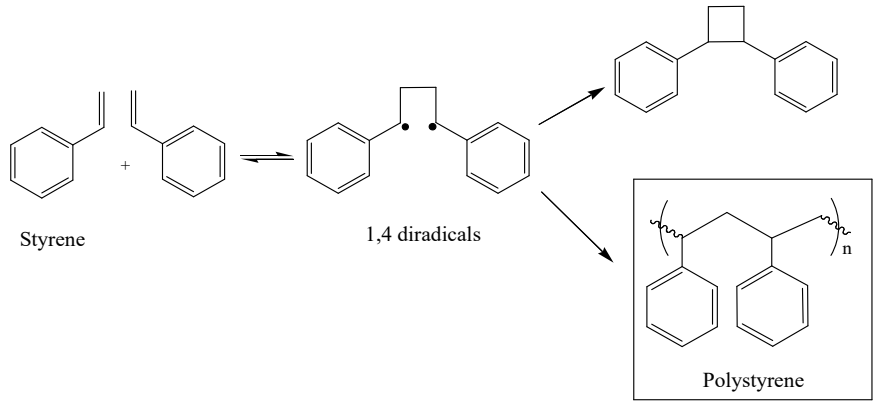

Figure 1.2.1. *Mechanism of PS polymerisation via free-radical polymerisation as proposed by P.J. Florey (1937).*

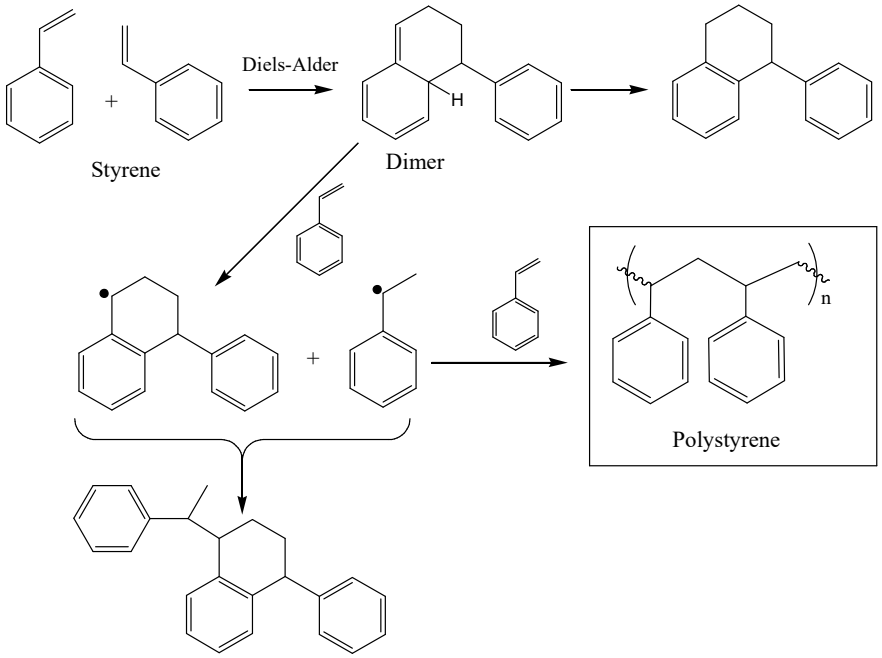

Figure 1.2.2. *Mechanism of PS polymerisation via free-radical polymerisation as proposed by F.R. Mayo (1968).*

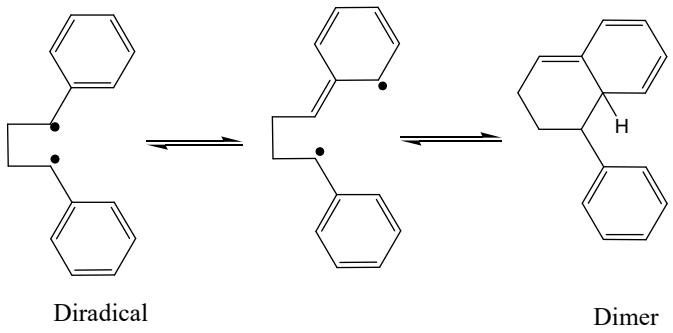

Figure 1.2.3. *Formation of dimer (F.R. Mayo) from diradical (P.J.Florey) as explained by J.Mulzer (1988)*

1.2.3. Classification of PS

Based on the production and processing techniques applied, different forms of PS could be obtained. These forms of PS differ from each other in physical, mechanical and electrical properties and hence in their applications too. General purpose polystyrene (GPPS), PS forms, expanded polystyrene (EPS), extruded polystyrene (XPS) and oriented polystyrene (OPS) cover these classifications.

- **General purpose polystyrene (GPPS):** These types of PS with $\bar{M}_w$ ranging between 2,00,000 to 3,00,000 are produced by free-radical polymerisation as discussed above. GPPS are hard and colourless. They have low specific gravity and are cheap. As the name implies, GPPS is the most common PS that we meet in our daily life for common usage. They are the type of PS hence produced by industries in large scale. They can be moulded into thin flexible films. They are electrical insulators and serve the purpose of insulation in electric devices too. GPPS is amorphous and has a glass transition temperature (T_g) around 100°C. GPPS could be moulded into various commodities of the users' choice, easily through injection moulding at a temperature below 200°C. GPPS has several disadvantages such as low heat resistant, low impact resistant and are soluble in some of the organic solvents. It should also be noted that the commercially available PS are not pure. They may contain oligomers of styrene and traces of initiators[33].

- **PS foams:** PS foams are made by the assembly of particles of PS containing air voids (volume fraction of air ≈8% and PS ≈2%). Suspension radical polymerisation is used to prepare PS beads, using blowing agents. The beads are subjected to steam and moulded to desired products. They serve the application of light weight water proof packing materials, insulators, surfboards etc. Insulating concrete form (ICF) that we see commonly is made up of PS forms. Structures like ornamental pillars that should be light weight are also made up of PS forms.

- **Expanded polystyrene (EPS):** are developed from pre-expanded beads of PS. They are very low dense white material, commonly termed as "Styrofoam". They are brittle and soft and are generally used as cushions to protect delicate appliances. The high thermal insulation property of EPS also makes them available for the use of packing frozen food items. They also serve as disposable plates and cups. Injection moulding is employed to manufacture the products of EPS.

- **Extruded polystyrene (XPS):** As the name implies, XPS are processed by extrusion method. Unlike EPS, XPS are closely packed and denser. They have a rough surface with reduced thermal conductivity. XPS finds their application in model making (especially architecture models).

- **Oriented polystyrene (OPS):** OPS are specially developed for packing purposes. XPS discussed above is opaque. On stretching XPS the haziness is reduced and transparency is increased. This is OPS. The advantage of OPS as packing material is that they are relatively cheap, at the same time stiff.

1.2.4. PS blends or copolymers

In order to enhance the properties of PS for specific applications, the PS is blended with some other polymers or molecules. Blending soft rubber with PS for example results in acrylonitrile-butadiene-styrene copolymer (ABS) and high impact polystyrene (HIPS) which shows superior impact resistance. ABS also shows enhanced chemical resistance. Styrene-acrylonitrile (SAN) obtained on copolymerization of styrene and acrylonitrile is resistant to chemicals and heat and also shows better mechanical properties.

1.3 Plastic Debris and environmental issues

1.3.1 Causes and consequences of plastic pollution

Increased consumption of plastic commodities including PS worldwide has led to a steep rise in the amount of plastic debris. The uncontrollable spread of plastic wastes which has adverse effects on the environment has become one of the primary concerns of most of the countries[37–39]. Plastics have touched almost all the sectors of human need replacing natural resources due to its magnificent properties. The use and throw system practiced by the humanity causes a huge deposit of hazardous PS debris have adverse effects on the bio system. Plastics like PS as we know are resistant to environmental weathering over a long period of time[40]. It takes a period of few decades for low density polymer materials like bags, wrappers etc., to degrade completely. Degradation of plastic bottles takes around half a millennium. Plastic products of higher size and density cost nearly a millennium to vanish completely from earth. This is of course too long for the bio systems of the environment. In

addition to this, studies are being conducted in order to increase the stability of polymers from environmental weathering[41–45]. Such polymers with incorporated stabilizers, further increases the life span of polymer debris. Some of the plastic debris ends up in land fillings. Lack of enough land for waste plastic deposition leads most of the debris exposed to the eco system and hence causing pollution.

Plastic which end up in the oceans are broken down and spread over a large area[46–49]. These debris are serious threat to the marine eco system and may even result in deaths of several marine life forms[50–53]. In addition to this various plasticizers added into the polymer matrix also contribute to the marine pollution[54–56]. Plastic debris spread over soil affects the soil fertility which has serious adverse effects on the bio system depended on soil[57–59]. Plastic debris are often unknowingly taken by animals and birds as food and are ingested causing various disorders or ultimate death[60,61]. The food safety of human being too is affected due to soil pollution caused by the plastic debris[62]. Plastic debris like PS forms or extruded PS are easily carried away by the wind to far-away places and spread the plastic pollution over a wider range.

1.3.2 Remedial measures against plastic pollution

Measures to treat pollution due to plastic debris are actively being thought of and implemented throughout the world. An effective method for plastic waste treatment is yet to be developed. Plastics cannot be banned all of a sudden as they have turned out to be a part of human life. The only way left is to find out a proper route to assemble the plastic debris and demolish them or recycle them at a very low cost.

In most cases, the primary idea for the demolition of plastic debris that originates in our mind is to burn plastics. Burning plastics is of course not a wise idea as the outcome of burning is toxic gases that can be lethal to the creatures including human beings who inhale them[63]. Burning plastics therefore results in air pollution. Controlled burning of plastics is done in municipalities or industries using incinerators. Incineration also produces acidic gases and other gases that lead to secondary air pollution causing various health issues. In addition to this, auxiliary fuels should be used for maintaining proper temperature that consumes energy[64,65].

Another method for the treatment of plastic wastes is recycling[66]. Even though this method sounds good theoretically, its scope is limited practically. The process called recycling is in fact a combination of several steps starting with the separation of plastic debris from other waste and sorting them (segregation). The next step is compaction which involves reduction in the volume of the plastics (up to 98% of the total volume). Shredding follows compaction where plastic pieces are changed into small flakes. Finally the flakes are pelletized using an extruder, melted and cooled. The resultant recycled plastics are used for manufacturing various commonly used commodities. The major disadvantage of recycling is its limited application and cost. Expanded polystyrene (EPS) for example occupies larger volume compared to its mass. This makes the transport of bulk EPS debris costly. The recycling process compresses EPS into smaller volumes. The recycled compressed EPS finally obtained does not worth much compared to the cost of recycling and transporting EPS. Another disadvantage of recycled PS is that it cannot be used for food storing/ packing for the sake of hygiene.

Biodegradation could not be thought of for polymers like PS, PVC, PE, PES, PP etc., as the enzymes of microbes are unable to digest these polymers. Polymers like PS could be degraded thermally[67].Thermal degradation of polymers is also not safe due to the formation of toxic gases and energy consumption. Chemical degradation[68] that is done in the presence of reagents could not be applied for large PS debris. The use of chemicals is not ecofriendly in some cases and is costly too. Radiolytic degradation is another effective process for the degradation of PS[69]. In this technique, the polymers are exposed to high energy gamma radiation. This technique too requires large amount of energy and are costly too. Photodegradation could be considered for the demolition of polymers as the process is cheap and ecofriendly. Methods to accelerate the process of photodegradation by loading it with suitable photocatalysts are being discussed in this thesis.

1.4 Photodegradation

Photodegradation refers to the decomposition of a material in the presence of electromagnetic radiations. Most of the polymers including PS undergo photodegradation in the presence of sunlight (mostly in the UV region)[70]. The main advantage of photodegradation over other methods of polymer remediation is that, it

is ecofriendly, cheap, produces no toxic gases and no artificial external energy is required (the process takes place in renewable natural sunlight). In simple words, we can call photodegradation, a "green" process. The disadvantage of photodegradation is that it takes long time for completion. Photodegradation depend upon the nature of polymers. High molecular weight polymers require a longer time to degrade completely and the samples should be exposed to more intense electromagnetic radiations.

1.4.1 Photodegradation of PS

PS undergoes photodegradation in the presence of UV radiation of the solar spectra. Photodegradation of PS is through photo-oxidation pathway in the presence of air. Slight yellowing is noticed as a result of photodegradation of PS due to the formation of conjugated double bonds that absorbs in the visible region. The mechanical properties of PS are deteriorated as a result of photodegradation. The flexibility of chain also decreases rendering it as a brittle useless material which is easily decomposed after photodegradation. Photodegradation of PS depends upon the mobility of ions through the matrix, impurities present within the polymer and interaction with atmospheric oxygen, water etc.

The phenyl rings which absorb UV radiations are excited to singlet followed by triplet states producing radicals initiating the degradation process. The degradation however depends upon the mobility of the radicals through the PS matrix. It should be noted that the mobility of radicals through solid phase via diffusion is hindered due to steric effect. Hydrogen radicals can find an easy way through the polymer matrix and interact with other molecules creating macromolecular radicals or combine with other hydrogen molecules or radicals. Bulky macromolecular radicals including the phenyl radicals cannot diffuse easily. These bulky molecular radicals however can abstract hydrogen radicals from their vicinity or can cleave the associated or neighbouring bonds leading to the relay of radical propagation until it is quenched[71]. The interaction of macromolecular radicals formed over the PS chain with the atmospheric gases or water molecules play a vital role in photo-oxidative degradation. Secondary radicals formed on interaction of macromolecular PS radicals with atmospheric oxygen or water molecules are responsible for oxidation over the PS chain. Formation of carbon-

carbon double bonds or conjugated double bonds due to cleavage of adjacent carbon-hydrogen bonds also results in oxidation.

The study of photodegradation of PS dated back in the 20th century. Matheson and Boyler in 1952 reported the yellow colouration on PS surface when exposed to light[72]. The yellow colouration of light exposed PS was due to the oxidation of PS leading to the affixation of some chromophoric groups according to the report. The formation of carbonyl groups on the PS chain upon light exposure was also reported. According to Matheson and Boyler, the yellow colouration of light exposed PS specimens could be washed off easily but they were not soluble in the solvents where PS was normally soluble. This could be due to the cross linking of PS polymer chains. In 1965 Grassie and Weir corrected the belief that the reason for yellowing of PS upon exposure to light was due to oxidation leading to the formation of colour absorbing groups[73]. According to the study, the formation of conjugated double bonds when PS was exposed to light radiation was responsible for the yellow colouration. Grassie and weir explained the theory of conjugated carbon-carbon double bond formation as illustrated below (Figure 1.3). UV radiation absorbed by the PS leads to the cleavage of α-C-H bond (marked as C_1) through homolytic fission. The hydrogen atom cleaved from C_1 now abstracts another hydrogen atom associated with the adjacent carbon atom (C_2) of the same chain. This ultimately leads to the formation of carbon-carbon double bond (>C=C<). The >C=C< formed between C_1 and C_2 renders the α-hydrogen (tertiary H atom) present on C_3 more labile. This triggers the homolytic cleavage of C-H bond (of C_2) followed by hydrogen abstraction from C_4 leading to the formation of >C=C< (between C_3 and C_4). Conjugated double bonds are thus formed. Three such conjugation results in the absorption of visible light (yellow region).

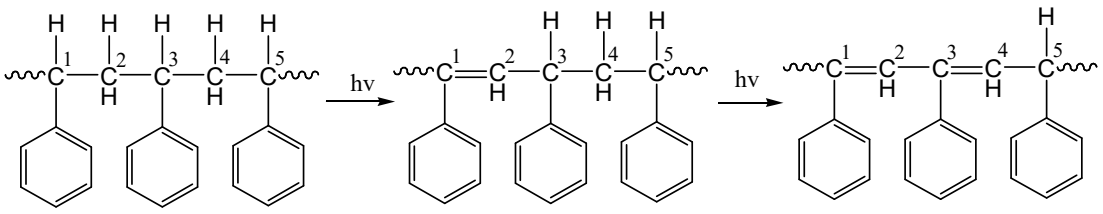

Figure 1.3. *Mechanism of conjugated double bond formation in PS chain under UV irradiation proposed by Grassie and Weir (1965)*

The intensity of the yellow colour is increased as a result of prolonged exposure to light radiations. However red shift to higher wavelength was not observed. This was explained by Grassie and weir by the limitation of extended conjugation due to the lack of coplanarity of PS matrix which restricts the mobility of molecules. George (1974) investigated the photodegradation of PS and reported that the presence of aromatic carbonyl groups as impurities in the PS matrix enhances the oxidation process[74]. Chain scission was observed in PS through Norrish type II reaction under UV exposure. Singlet oxygen was formed when UV radiation interacted with the impurities or air which further attacks the PS chain leading to the introduction of hydroperoxy group in the chain. The increase in the intensity of >C=O absorption bands in the IR spectra of PS upon UV irradiation was observed. The effect of temperature on photodegradation was studied by Torikai et al. (1986)[75]. The degradation of PS was studied under a mercury lamp at temperatures 30°C, 100°C and 120°C which were below, equal to and above the glass transition temperature (T_g) of PS respectively. Photo-oxidation increased as the temperature increased. The concentration of polystyryl radicals formed initially decreased as the temperature increased. The conclusion was that, at higher temperatures, cross linking between the adjacent chains of PS matrix resulted by the combination of polystyryl radicals assisted by the segmental motion of the chains.

Photodegradation as explained is a slow process. Photodegradation could be implemented as a common system of plastic waste treatment only if the entire process proceeds in a stipulated amount of time. Introducing photocatalysts/ photosensitizers that could efficiently accelerate photodegradation has been thought of and investigated by many researchers worldwide.

Acceleration in polymer degradation could be achieved by the use of metal oxides[76–79], modified metal oxides[80], organic photosensitisers[81–84] etc. loaded into the polymer matrix. Of late the enhancement of photodegradation of polymers coupled systems like metal doped metal oxides[85], organo-inorganic systems[80] etc. is also being studied. Photodegradation studies have also been done by modifying the chain of a particular polymer by copolymerizing it with another polymer [86]. It has been observed that inorganic metal oxide semiconductors like TiO_2, ZnO etc showed superior photocatalytic activity. Our study presented in this thesis includes the

photodegradation of PS in the presence of nano TiO_2 as well as TiO_2-photosensitizer couples under UV radiation. TiO_2 have been chosen as core catalyst in this work, considering its superior photocatalytic activity, photostability, non toxicity, ease of preparation and better thermal stability. ZnO and photosensitizer-coupled ZnO have also been used in our study. Importance has been given to TiO_2 however considering superior photocatalytic activity and photostability of TiO_2 compared to ZnO.

1.5 Titanium dioxide (TiO_2)

TiO_2- an oxide of the transition metal titanium, has been commercialized in 1920s since its discovery by William Gregor in 1791 in black magnetic sand followed by its isolation from the mineral rutile by Klaproth in 1795. The first products developed out of TiO_2 were pigments[87]. The application of TiO_2 has extended from the level of pigments to that of a catalyst within a short span of time[88,89]. One notable work includes the study of Fujishima and Honda (1971) who used TiO_2 as an anode in the electrochemical photolysis of water[90]. The use of TiO_2 has increased commercially as well as in catalysis in the following years.

1.5.1 Polymorphs of TiO_2

TiO_2 exists in three different morphologies namely anatase, rutile and brookite. These three polymorphs differ by the sequence in which the TiO_6 octahedral units are arranged (Figure 1.4). Anatase and rutile phases are used in photocatalysis[91]. Anatase phase shows superior photocatalytic activity compared to rutile phase TiO_2[92].

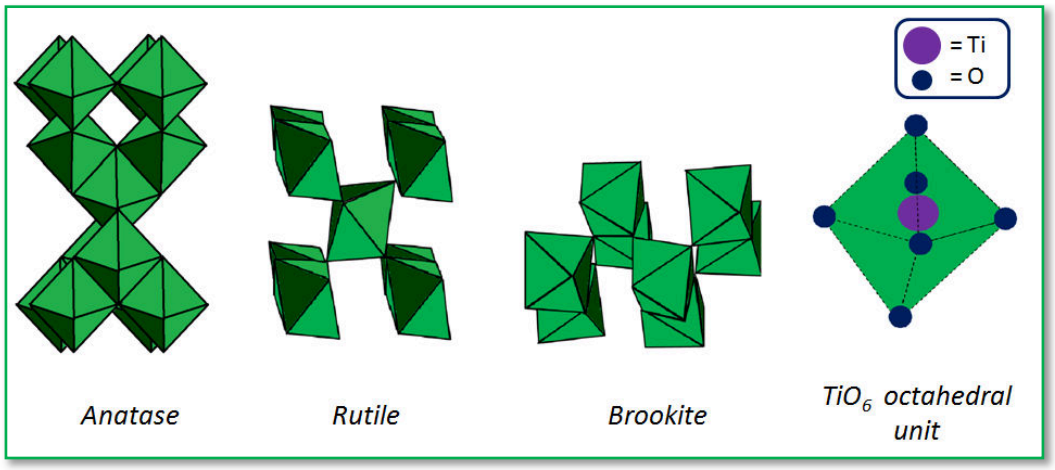

Figure 1.4. *Arrangement of TiO_2 octahedral units in anatase, rutile and brookite polymorphs of TiO_2*

TiO_2 also have several metastable forms such as hollandite oxide ($TiO_2(H)$)[93], TiO_2 (B)[94] and ramsdellite type ($TiO_2(R)$)[95] structures. TiO_2 also exists in high pressure forms namely cubic[96], orthorhombic columbite (TiO_2 II)[97] type, intermediate orthorhombic (TiO_2 OI)[98], orthorhombic cotunnite (TiO_2 OII)[99] type, and monoclinic baddeleyite (MI) type[100] structures. TiO_2 OII with cotunnite $PbCl_2$ like structure holds the credit of being the hardest oxide known. When octahedral TiO_6 (O_h symmetry) units combine in different ways to form different oxides of titanium, a distortion in its regular octahedral structure occurs. This leads to a change in O_h symmetry of the TiO_6 units. As a consequence of the distortion in the regular O_h symmetry of TiO_6 units, further splitting in the t_2g and e_g bands are observed in the electronic spectra as sub-bands[101]. The perfect O_h symmetry of TiO_6 (as observed in cubic structure) undergoes tetragonal distortion into D_{2d} symmetry in anatase and D_{2h} symmetry in rutile structures. Similar distortions are observed in other structures (say Ti_2O_3 → trigonal distortion; Ti_4O_7 & Ti_5O_9→ orthorhombic distortion and so on). The splitting patterns of octahedral, tetragonal, trigonal and orthorhombic symmetries are as represented below (Figure 1.5)[102].

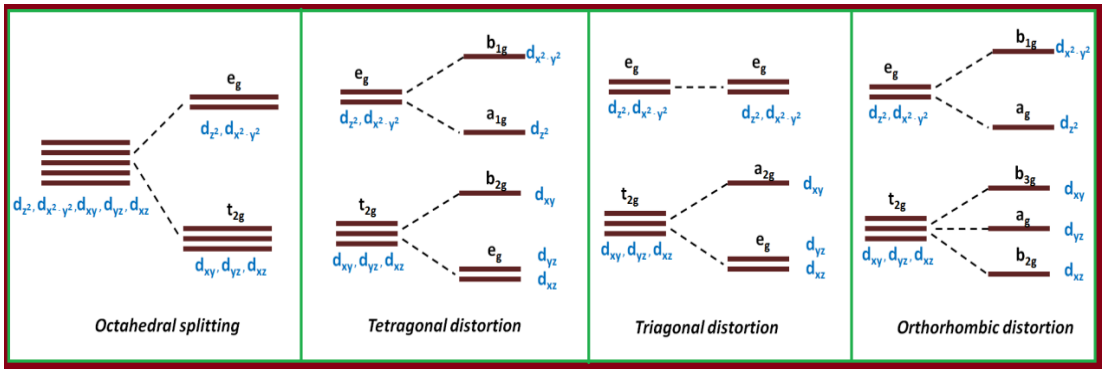

Figure 1.5. *Bands and sub-bands in the electronic structure due to octahedral splitting, tetragonal, trigonal and orthorhombic distortions*

1.5.2 General methods for TiO_2 synthesis

TiO_2 was reported to be synthesised using several methods. Some methods employed for the synthesis of TiO_2 are discussed below.

- **Sol-gel method**

In sol-gel method, the precursor used for the preparation of a particular compound is hydrolysed in solution to form sols. These sols are then transformed into gel on

polymerisation. The gel so formed is transformed into products on heat treatment. TiO_2 have been synthesised through sol-gel technique from Ti(IV) alkoxides in acidic pH[103–105]. The amount of water used in the process controls the hydrolysis rate and thereby the structure of TiO_2 formed. When the water content is less in the reaction mixture (titanium alkoxide is in excess) the rate of hydrolysis will be lower facilitating the growth of Ti-O-Ti chains. The growth of Ti-O-Ti would be in such a way that close packed three dimensional structures are formed. In the reaction mixture where the amount of water is comparatively higher, the rate of hydrolysis would also be higher favouring the development of $Ti(OH)_4$ which ultimately results in particles which are loosely packed (first order particles). This is due to the fact that three dimensional structures of Ti-O-Ti are not developed appreciably in the intermediate step. When the water content in the reaction mixture is in excess the growth of three dimensional Ti-O-Ti chains in the gel are favoured resulting in first ordered particles that are closely packed[106–108].

Sugimoto et al. have conducted several studies regarding the synthesis of TiO_2 through sol-gel route. The precursor used was titanium(IV) isopropoxide (TTIP) mixed with triethanolamine (TEOA) in the ratio 1:2. Amines were used as surfactants that controlled the shape of the particles. pH of the system was tuned and it was found that the shape of nano TiO_2 at acidic pH was cuboidal and at basic pH (above 11) it was ellipsoidal. When TEOA was replaced with diethylenetriamine, ellipsoidal shape was obtained at a pH just above 9[109–111]. Sodium oleate and Sodium stearate used in the reaction mixture could tune the shape of the TiO_2 particles from distorted cubes to perfect cubes having sharp edges[110]. The studies of Uekawa et al. (2002)[112] and Le et al (2004)[113] showed that the agglomeration of TiO_2 particles could be prevented during the crystallisation process by heating the gel to a temperature below 100° C for a prolonged time. Zhang and Banfiled obtained anatase nano TiO_2 with size below 50 nm by heating amorphous TiO_2 aerobically in the series of their work done on TiO_2 synthesis through sol-gel route[114–117]. In order to obtain TiO_2 particles of high crystallinity, Kim et al.[118,119] modified the sol-gel method as continuous reaction as well as two stages mixing methods. Znaidi et al. (2001) on the other hand adopted semicontinuous method for the same purpose[118]. Synthesis of TiO_2 nano tubes were also reported by several authors using sol-gel route[120–122].

- **Hydrothermal method**

The advantage of hydrothermal method is that the temperature of the aqueous reaction mixture can be elevated much above 100° C (>boiling point of water) at an elevated pressure. The morphology and size of the product formed can be controlled by adjusting the parameters such as reaction temperature and the quantity of solvent used. The process is done using steel hydrothermal autoclaves (which may or may not be teflon lined). Many authors have reported the synthesis of nano TiO_2 particles using hydrothermal technique[123–125]. Yang et al. (2001) for example reported the synthesis of nano TiO_2 by subjecting the peptized precursor of TiO_2 to hydrothermal process[126]. Chae et al. (2003) reported the synthesis of TiO_2 by the hydrothermal treatment of titanium alkoxide in ethanol water mixture adjusting to acidic pH[125]. Hydrothermal method have also been adopted for the synthesis of nano rods[127–129], nano wires and nano tubes[130,131]. Zhang et al. (2002) reported the conversion of TiO_2 particles into TiO_2 nano wires by treating it with NaOH hydrothermally at a temperature range 150-200°C[132]. Wei et al. (2004) synthesised TiO_2 nano wires from layered titanate[133]. Kasuga et al. were the first to introduce the synthesis of TiO_2 nano tubes through hydrothermal process in (1998)[134]. Nano tubes were also developed from the hydrothermal process of TiO_2 powder in the presence of NaOH. An interesting mechanism was suggested by Kasuga et al. in 1999 for the formation of TiO_2 rods[135]. NaOH treatment leads to the cleavage of Ti-O-Ti bonds of TiO_2 leading to the formation of Ti-O-Na as well as Ti-O-H bonds. Reaction of these newly formed bonds with water and HCl results in the formation of sheets of Ti-O-H linkage which on dehydration converts into Ti-O-H-O-Ti sheets. These sheets finally folds to form TiO_2 tubes.

- **Solvothermal method**

The difference between hydrothermal and solvothermal processes lies in the solvent used during the course of reaction. When aqueous medium used in hydrothermal process is replaced by organic solvents, the process is called solvothermal process. The advantage of solvothermal process over hydrothermal process is that the temperature of the system could be elevated much higher than that of hydrothermal process depending upon the solvents chosen. As a result of this the

particles produced via solvothermal approach could be better controlled in their size, shape and distribution compared to the product of hydrothermal synthesis.

Several authors have reported the synthesis of nano TiO_2 (particles, rods etc) using solvothermal methods[136,137]. Kim et al. (2003) used toluene as the solvent for the preparation of TiO_2 from TTIP precursor at a temperature of 250°C by solvothermal method[138]. Li et al. (2006) prepared TiO_2 nano particles and rods from titanium tetraisobutoxide precursor using linoleic acid as solvent[139]. TiO_2 nano rods were synthesised from TTIP precursor in toluene solvent and surfactants at 250° C by Kim et al. (2003)[140]. TiO_2 nano wires have also been prepared using solvothermal method[136,141]. The TiO_2 rods and NaOH were autoclaved in ethanol-water mixture at temperature between 170 and 200°C (Wen et al. 2005)[141].

- **Chemical vapour deposition (CVD) method**

Materials are converted into vapour state followed by condensation to obtain the required product in CVD approach. CVD is a versatile method adopted for the preparation of coated materials over a substrate. Surface coating of substrates with other materials are employed in varied applications to tune their electrical, corrosion resistant, optical, thermal etc. properties. Other than for coating purpose, CVD method is employed for the preparation of nano particles, fibers, films etc.

TiO_2 has been prepared using CVD in oxygen-helium atmosphere from TTIP precursor (Seifried et al; 2000)[142]. Sung et al (2018) used CVD for TiO_2 ultrathin coating on boron particles from TTIP[143]. Alotaibi et al. (2018) synthesised TiO_2 brookite thin films and found that its photocatalytic activity was superior compared to anatase TiO_2 particles[144]. Nagasawa et al. (2018) prepared TiO_2-coated polymethylmethacrylate polymer which exhibited excellent UV shielding effect[145].

- **Sonochemical method**

Sonochemistry utilizes the acoustic cavitation originating from the interference of ultrasound with reaction media. High pressures and localized heat results as a consequence of the bubbles formed during cavitation. This in turn drives a chemical reaction through improved interaction between the molecules. Nano TiO_2 has been synthesised using sonochemical method[146,147]. Huang et al. (2000) synthesised

anatase, rutile and mixed phase nano TiO_2 using different precursors at varying temperature by sonochemical method[146]. TiO_2 nanotubes were prepared through sonochemical method by Zhu et al. (2001) by sonicating TiO_2 in the presence of NaOH[147]. Yu et al. (2001) sonicated TTIP in ethanol water mixture and reported the formation of TiO_2 with a mixture of anatase and brookite phases that exhibited photocatalytic activity[148].

1.5.3 TiO_2 as a photocatalyst

TiO_2 is a well celebrated photocatalyst used in various applications related to energy conversions, water purification, air purification, defogging, hydrogen generation, self-cleaning, sterilization etc. What makes TiO_2 such a satisfying photocatalyst is its superior efficiency, non-toxicity, photostability, ease for synthesis and low cost compared to other metal oxides[149–151].

TiO_2 is a semiconductor metal oxide having a band gap energy (E_g) above 3.0 eV (band gap varies in different polymorphs of TiO_2 and also depends upon the particle size). Such a large value of E_g restricts its absorbance to the UV region of spectra. UV irradiation of TiO_2 results in the formation of electron-hole pairs (if $h\upsilon \geq E_g$). The photogenerated electrons in the valence band (VB) are transferred into the conduction band (CB) through the band gap leaving behind positive charged holes in the VB. The photocatalytic activity of TiO_2 depends upon the fate of these photogenerated electrons and holes. The electron in the VB interacts with the adsorbed oxygen leading to the formation of reactive superoxide ($O_2^{\bullet -}$). The holes left behind in the CB on the other hand react with adsorbed water or hydroxyl ion (OH^-) to form reactive hydroxyl radical OH•[152–154]. The $O_2^{\bullet -}$ and OH• further interacts with the reactant molecules including polymers, pollutants etc. if present in their vicinity to initiate various reactions[155]. If polymers like PS, are attacked by these reactive radical species, oxidation of the polymer chain takes place. In such cases >C=O, -OH and -OOH groups are introduced in the polymer chain termed as photo-oxidation[156]. It should also be noted that all these possible reactions occur if the photo generated electrons and holes either have appreciable life time or they are transferred into another system associated with TiO_2. If the photo generated charges recombine before having a chance for the interaction with other molecules, the photocatalytic activity is

quenched. The entire mechanism of photocatalysis of TiO_2 is pictorially depicted in Figure 1.6.

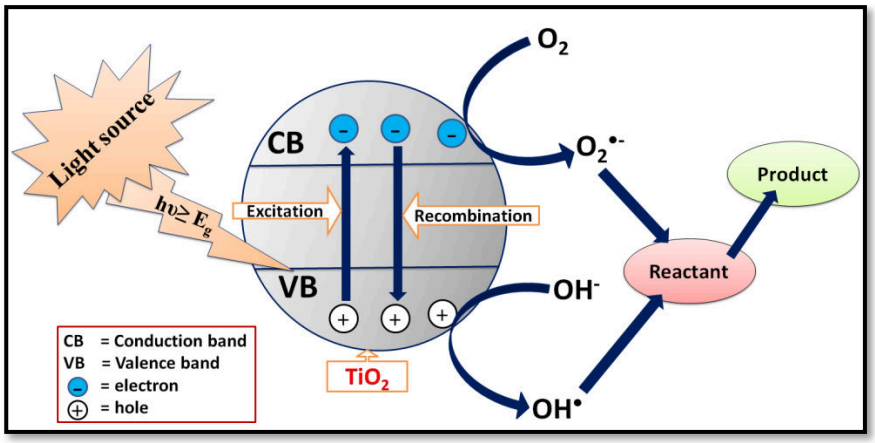

Figure 1.6. *Mechanism of photocatalysis of TiO_2*

The holes left behind in the VB may not combine with water directly in all the cases. They may get trapped in the oxygen sites within TiO_2 and may weaken the Ti-O bond existing in the lattice. The adsorbed water molecules now get a chance to react with these loosely bounded Ti-O bonds leading to the formation of -OH groups on the surface of TiO_2 through coordination. These less stable bonds make the TiO_2 surface superhydrophilic[157].

Table 1.1. *Expected properties of TiO_2 related to its structural dimensionality*

Structures	Names	Dimensions	Properties
	spheres	0D	• High surface area
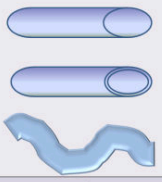	Rods Tubes Wires	1D	• Delayed charge recombination. • Light scattering. • Fabricated into nonwoven mat
	Sheets	2D	• High adhesion. • Smooth surface.
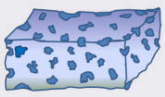	Interconnected structures	3D	• Better mobility of charge carriers.

The structure of TiO_2 assembly exhibits variant properties suitable for different choice of photocatalytic application. Zero-dimensional (0D) TiO_2 nano spheres, for

example, due to its high surface area could be used in photocatalytic decomposition/ photodegradation of pollutants[158]. One-dimensional (1D) TiO_2 rods, tubes and fibers show better light scattering[159] and delayed electron-hole recombination[160] properties. The enhanced diffusion of charge carriers in these 1D structures is the reason for this delayed recombination of charges[160]. They also could be fabricated into mats which are self stabilised[161]. Two-dimensional (2D) TiO_2 sheets have the characteristic property of high adhesion with smooth surface[162]. Three-dimensional (3D) structures of TiO_2 bears interconnected architecture that enables easy mobility of charge carriers. 3D TiO_2 monoliths find their application in environmental purification[157].

TiO_2 is being widely used as photocatalyst in water treatment for the degradation of various contaminants. Organic dyes exposed to water could be successively removed using TiO_2 photocatalyst in the presence of UV light. These dyes include Procion yellow H-ELX[163], Methylene blue[164], Amaranth[165], acridine orange[166] etc whose removal efficiency depended upon pH. An enhancement in the dye removal using TiO_2 was achieved by the addition of H_2O_2 for dyes like Rodhamin 6G[167], direct dye 40 [168], etc. Tang et al. reported that the increase in azo linkage decreased the rate of dye degradation in the presence of TiO_2 catalyst and UV radiation. The rate of degradation of the azo dyes followed the order Direct blue 87 > Basic Yellow 15 > Acid Blue 40[169]. The degradation of Reactive Black 5 under UV irradiation and TiO_2 increased in the presence of dissolved oxygen and NaCl, and was independent of pH[170]. An inhibition in the degradation of Reactive Red 198 dye was reported in the presence of ethanol[171]. Photodegradation of some phenolic compounds including phenol [172–174], 2-chlorophenol[175], 2,4-dinitrophenol[176], bisphenol A[177,178] in the presence of TiO_2 and application of TiO_2 based on its superhydrophilicity[179–181] and wettability[182,183] has also been reported.

TiO_2 has also been used as catalyst in polymer degradation with appreciable results. Cho and Choi (2001)[184] studied the photodegradation of PVC in the presence of TiO_2 under UV radiation of wavelength (λ) 300 nm and ambient supply of air. PVC-TiO_2 composite underwent better photodegradation compared to pure PVC. Mass loss, decrease in average molecular weights, increase in the formation of carbonyl groups and evolution of CO_2 and water vapour upon UV irradiation was monitored. Photodegradation of polyethylene (PE) loaded with TiO_2 under solar light

and artificial UV radiation in ambient air supply was investigated by Zhao et al. (2007)[185]. The photodegradation of PE increased as the percentage of TiO_2 loading increased with the evolution of CO_2 and water. The degradation initiated in the PE-TiO_2 interface was extended over the PS matrix. The reactive oxygen produced on TiO_2 photocatalyst diffused through the PE matrix causing the oxidative- degradation of rest of the PE chain. Thomas et al. (2013)[186] reported that the size of TiO_2 photocatalyst used, affected the rate of photodegradation of low density polyethylene under UV radiation. TiO_2 with smaller particle size exhibited better photocatalytic activity compared to the larger sized TiO_2. The photodegradation of polycarbonate (PC) in the presence of TiO_2 as reported by Hwang et al. (2014)[76] resulted in various side products including aliphatic and aromatic ketones. The weight loss observed in the PC-TiO_2 composite was double as observed in pristine PC under UV irradiation. Shang et al. (2003) studied the photodegradation of PS-TiO_2 composites under UV radiation and observed better photo-oxidation, weight loss, decrease in molecular weight etc. for the composites compared to pristine PS[187]. Diffusion of reactive oxygen- by the interaction of photogenerated electrons in TiO_2, through the PS matrix extended the range of degradation along the PS chain. In 2011, Jaleh et al. investigated the photodegradation of spin coated PS-TiO_2 composite films and reported that the hydrophilicity and contact angles were affected by photodegradation process[188].

1.6 Modified TiO_2 for enhanced photocatalysis

TiO_2 is a versatile photocatalyst used in many areas including environmental and energy related applications. The full-fledged photocatalytic activity of TiO_2 however cannot be utilised due to its rapid charge recombination. The meagre response of TiO_2 towards visible spectra too limits its application. It should be noted that TiO_2 is photo catalytically active only in the UV region of the spectra that comprises only about 3 to 5% of the total radiation reaching the earth. In addition to this, the photocatalytic efficiency of TiO_2 also depends on the separation of photo carriers and their transportation to the reactant associated with TiO_2. Weaker separation efficiency also restricts its photocatalytical activity[189]. In order to overcome these limitations of TiO_2, modifications are done. Modification refers to the processes like doping, sensitizing, composite fabrication etc. Modification of TiO_2 reduces the possibility of charge

recombination and/or narrows the band gap energy. When charge recombination is delayed, better photocatalytic activity is exhibited by TiO_2 and modifying TiO_2 with suitable materials extends its activity to the visible region of the spectra[190].

1.6.1 Metal doping

Some of the methods adopted for the preparation of metal doped TiO_2 include hydrothermal[191,192], sol-gel[193,194], sol-gel/microemulsion[195], impregnation[196], impregnation/photodeposition[197], photochemical deposition[198], photochemical reduction[199], reflux[200] etc. Many studies have been done on the structure and properties of TiO_2 doped with alkaline metals[201], alkaline earth metals[202], 3d-transition metals[203],4d-transition metals[204] and rare earth metals[205]. All the studies showed that the enhancement in the photocatalytic property of metal-doped TiO_2 could be achieved by lower concentration of metal doping (<10%). Metal doping facilitates the transport of photogenerated electrons from the CB into the metal. Redox potential of the radical species created during photocatalysis at the vicinity of TiO_2 is increased as a consequence of metal doping. These species can easily trigger photochemical reactions, reducing the time of charge recombination within TiO_2[206].

Transition metal doped TiO_2 has been most widely used by various research groups in several applications especially environmental purification. Transition metals can disturb the electronic properties of TiO_2 causing a shift in its absorption from UV to visible region. The photocatalyst so developed using transition metal doped TiO_2 may be active in the visible region too[207]. Inturi et al. (2014)[208] studied the photocatalytic efficiency of transition metals V, Cr, Mn, Fe, Co, Ni, Cu, Mo, Y, Ce, or Zr doped TiO_2. Better conversion in the visible region was observed in V, Cr or Fe doped TiO_2. The photocatalytic activity of Cr doped TiO_2 was found to be superior compared to TiO_2 doped with other metals. Doping Cr with TiO_2 increased the reduction potential of Ti and Cr leading to the formation of Ti-O-Cr bond that increased the photo response of the system.

Several authors have reported the enhancement in the photocatalytic activity of metal doped TiO_2 for the removal of environmental pollutants [193,209,218,210–217]. Mogal et al. (2014)[219] conducted a detailed study with regards to the structure of Ag-doped TiO_2 of varying Ag concentrations and its efficiency for the photodegradation of

phthalic acid under UV radiation. Even at 0.75% Ag doping, better thermal stability and degradation efficiency was achieved for Ag-TiO_2. Increased Ag doping percentage decreased the photocatalytic efficiency of Ag-TiO_2. Ag metal was found to agglomerate at the surface of TiO_2 as the percentage of Ag doping increased. Chiang et al. (2002) reported the oxidative degradation of cyanide ions using Cu doped TiO_2 catalysts with different Cu doping percentage under UV radiation. The rate of oxidation of cyanide was maximum at 0.1 % Cu doping and higher percentage of Cu retarded the reaction[220]. Superhydrophilic Cu doped TiO_2 catalysed photodegradation of Methylene blue was reported by Wang et al (2014)[221]. The Cu doped TiO_2 also exhibited antifogging property.

1.6.2 TiO_2 modified by carbonaceous materials

Carbonaceous compounds like activated carbons[222,223], carbon nanotubes (CNTs)[224,225], fullerene[226], graphenes/ graphene oxides[227,228] are used to modify TiO_2 photocatalyst owing to the unique properties exhibited by them. The advantages of such carbonaceous compounds modified TiO_2 lie on their special abilities to tune the electrical, structural and optical properties. Such composites are observed to exhibit superior chemical and thermal stability too[229,230]. Another advantage of carbonaceous compounds lies in their ability to hold TiO_2 within their matrix taking advantage of their large surface area. Better transfer of charge carriers along their surface is also facilitated[231]. The application of carbonaceous materials modified TiO_2 photocatalysts depend on the type of carbon structure used as different carbon allotropes have their own unique properties. Enhancement in the mechanism of photocatalytic activity of TiO_2 coupled carbonaceous materials lie in their superior adsorption property[232]. The carbon materials can adsorb various dyes like ecotoxic pollutants on their surface and can relay the photogenerated charge carriers originating from TiO_2 to these pollutants[233]. Ti-O-C bonds could be formed in the TiO_2 coupled with carbonaceous compounds[228,234,235] thereby extending their photo response towards the visible region[236]. Carbon materials also play the role of electron reservoirs that accepts and stores the photogenerated electrons from the CB of TiO_2 thus reducing the chance of electron hole recombination within TiO_2[237]. The electrons stored in the carbon materials associated with TiO_2 are utilized for the photochemical process.

Activated carbons have the special property of high surface area due to its porous nature. The pores could be classified as micro, meso and macro depending on the sizes. This porous nature helps activated carbon to adsorb impurities on its surface. Zhang et al. (2004) reported an interesting scheme by which municipal sewage sludge was utilized for the development of activated carbon. The activated carbon so developed was coupled with TiO_2 for the removal of Hg(II) ions from contaminated water photochemically. The TiO_2-activated carbon photocatalyst adsorbed the Hg(II) ions and reduced them into Hg(0) which was then recovered from the solution[222]. Wang et al. (2007)[223] prepared TiO_2-activated carbon couple by developing TiO_2 crystals over activated carbon. The photocatalyst so produced through sol-gel technique exhibited an appreciable activity in the UV region for the photodegradation of Chromotrope 2R in aqueous media. Activated carbon was coated on the surface of TiO_2 via hydrolytic precipitation method by Li and coworkers (2006)[238] using tetrabutylorthotitanate as precursor. The modified TiO_2 so produced showed enhanced photochemical activity for the degradation of methyl orange obeying pseudo-first order rate law. Deqing Mo and Dai Qi Ye. (2009) devised a setup by which activated carbon fibers were first modified using nitrogen plasma followed by loading it with TiO_2. TiO_2 loading into the developed carbon fibers was accomplished using tertiary butyl titanate via hydrolysis. The photocatalyst so produced could degrade formaldehyde much efficiently[239]. Slimen et al. (2011)[240] further heated TiO_2-activated carbon composite in air at 700°C which was developed through sol-gel technique. The photocatalyst was used for the degradation of methyl orange under visible light irradiation. Orha et al. (2017)[241] adopted microwave supported hydrothermal process for the preparation of granular activated carbon modified TiO_2. The photocatalyst so developed actively degraded humic acid under UV radiation.

Carbon nanotubes (CNT) with its one-dimensional rolled network like structure offer better surface area. They can stabilise TiO_2 associated with them. The properties of CNT could be tuned by functionalisation. Better thermal and electronic properties are exhibited by CNTs[242]. CNTs could be classified based upon the number of the of concentric carbon network rolled to form tubes. Single walled carbon nano tubes (SWCNTs) and multi walled carbon nanotubes (MWCNTs) consist of single carbon tube and multiple concentric carbon tubes rolls respectively[243]. Better photosensitization is promised by CNTs coupled with TiO_2 structures.

Yen et al. (2008) reported that the photocatalytic activity of TiO_2-MWCNT photocatalyst prepared through sol-gel route was found to be superior to those synthesised through hydrothermal route for the photodegradation of NOx and phenol[244]. Sol gel process was used by Gao and co-workers (2009)[245] to coat anatase mesoporous TiO_2 nano layers over MWCNT. Uniform coating of TiO_2 over MWCNT was accomplished with the air of surfactants. The developed photocatalyst showed improved efficiency for the photodegradation of methylene blue. Ashkarran and co-workers (2015)[246] developed TiO_2-CNT composites via different approaches like simple mixing, mixing followed by heating and mixing followed by UV irradiation. The UV irradiated composite exhibited superior photocatalytic activity compared to the others. TiO_2-CNT nano fibers were prepared by Wongaree et al. (2016)[247] using electrospinning method which showed effective activity for the photodegradation of methylene blue and benzene gas. Ahmad et al (2017)[248] prepared hair like TiO_2-CNT wires via CVD technique that could completely degrade methyl orange solution from the aqueous solution within 30 minutes.

The most widely used type of fullerene for photocatalytic applications is C_{60} with 60 p-electrons and C_{70} with 70 p-electrons[249]. C_{70} is less symmetric compared to C_{60}. As result of this, better ability for free radical creation is observed in C_{70} compared to C_{60}. Electron affinity of C_{70} is higher compared to C_{60} [250]. Superior visible light response observed in C_{70} compared to C_{60} could be explained by its larger photo cross-sectional area[251]. Most of the studies are however based on C_{60} TiO_2 couple. C_{70} has been into the picture recently. The conjugated close-shell structure with delocalised electrons has added to its unique physicochemical properties[252,253]. Fullerenes can act as sensitizer when coupled with materials like TiO_2 separating the photogenerated charge carriers much efficiently[254]. This is accomplished by its electron accepting property[254]. They can absorb mainly in UV region and moderately in the visible region[255]. The properties of fullerene can further be tuned by functionalisation.

Arrays of TiO_2-fullerene nanotubes[256], TiO_2-fullerene prepared via refluxing method[257] and TiO_2-fullerene prepared via hydrothermal method[258] were reported to show better photocatalytic property for the photodegradation of Methylene blue, Cr(IV) and Rhodamine B. Functionalised fullerene-TiO_2 composites like water

soluble polyhydroxyl fullerene coupled with TiO_2[259] and carboxylic acid functionalized fullerene coupled with TiO_2[260] efficiently degraded Procion red and Rhodamine B dyes photochemically. Out of these the carboxylic acid functionalized fullerene could shift the photocatalytic activity of TiO_2 towards visible region and the degradation of Rhodamine B took place under the visible light. Monolayer dispersion of C_{60} over mesoporous TiO_2 was achieved by hydrothermal method as reported by Yu et al. (2011)[261] which catalysed acetone oxidation. Qi and co-workers[262] reported that the optimum loading of 2% C_{60} into TiO_2 prepared through solution phase method catalysed the photodegradation of Methylene blue more efficiently. A comparison between the photocatalytic activities of C_{60} and C_{70} coupled with TiO_2 was made by Cho and co-workers (2015)[263] for the photodegradation of Methylene blue. C_{70} incorporated TiO_2 was found to show better activity for the photodegradation of Methylene blue under visible light irradiation.

Graphene is another significant material which is widely being studied accounting its outstanding unique properties. The sp^2 hybridized two dimensional hexagonal array of carbon atoms could be extracted from graphite[264]. In fact graphene is nothing but a single layer 2D sheet exfoliated from 3D structured graphite by chemical or physical methods[264]. Graphene has been of quite interest for the researchers owing to its electrical[265,266], mechanical[267], interfacial[268], photosensitizing[227], capacitance[269] and thermal[270] properties. Graphene also have high charge mobility along its structure[265]. Graphene find application in photocatalysis[271], composite materials[272], medicine[273], energy conversions[274], electronic devices[275], molecular sensors[276], liquid crystal devices[277], quantum hall devices[278], ultracapacitors [279] etc. The properties of graphene are quite tunable by doping[280] and functionalisation[281].

Graphene oxide (GO) as the name implies, is the oxidized form of graphene. In GO the oxygen atoms are bonded covalently to some of its carbon atoms resulting in the formation of hydroxyl or epoxy bonds[282–286]. Peripheral carbon atoms in GO may also contain carboxylic acid functional groups attached in addition to hydroxyl and epoxy groups[287]. The presence of these functional groups decrease the delocalisation of electrons through the graphene backbone of GO[288] and increase the hydrophilicity of the material. GO is in fact highly dispersible in water whereas graphene is not [234,289]. Hummers method[290] is most widely used for the preparation of graphene oxide

(GO) from graphite. During the process, oxidising agents used (H_2SO_4, $NaNO_3$ and $KMnO_4$) penetrate through the graphite layer and oxidizes the layers of graphite. This weakens the bond between each layers of graphite[291]. Process like sonication can lead to exfoliation of each layers into GO. The GO hence formed can be reduced into reduced graphene oxide (rGO) using simple chemical process. UV irradiation of GO catalysed by TiO_2 in ethanol media can also reduce it into rGO[289].

Zhang et al. (2011)[271] compared the photocatalytic activity of TiO_2-graphene and TiO_2-CNT photocatalysts for the selective oxidation of alcohols. Better photocatalytic efficiency was observed in TiO_2-graphene composites compared to that of TiO_2-CNT. The photocatalytic activity of TiO_2 was further tuned by controlling the morphology of TiO_2-graphene composite. Huang et al. (2013)[292] reported that the enhanced photocatalytic activity exhibited by TiO_2-graphene for the photodegradation of formaldehyde in air was due to the formation of Ti-C bond between TiO_2 and graphene. The formation of Ti-C bond facilitated the easy charge transfer from TiO_2 to graphene thereby reducing the charge recombination in TiO_2. Liu and co-workers (2013)[228] developed a core shell structure in which TiO_2 was encapsulated by GO. The condensation reaction between the -OH groups on TiO_2 surface and -COOH functional groups on GO resulted in the core shell structure. Enhanced photodegradation of Rhodamine B dye under UV as well as visible light was observed in the presence of the core shell TiO_2-GO structure, compared to pure TiO_2 photocatalyst. Umrao et al. (2014)[293] reported that the formation of Ti-O-C between TiO_2 and graphene in TiO_2-graphene composite minimised its band gap energy. The easy movement of charge carriers along the Ti-O-C bridge between TiO_2 resulted in better electron-hole separation and lowering of band gap energy. The composite catalysed the photodegradation of Methylene blue dye under visible light radiation. Rakkesh et al. (2014)[294] studied the photodegradation of Methylene blue dye catalysed by TiO_2-graphene and ZnO-graphene photocatalysts. Both the photocatalysts exhibited better efficiency for the photodegradation of the dye in sunlight due to the formation of heterojunction between the metal oxides and graphene. Increased interfacial charge transfer resulted in better electron hole separation in TiO_2 as well as ZnO in the presence of graphene. Hi and co-workers (2016)[295] developed bipyramidal structured TiO_2-rGO photocatalyst. The structure

consisted of one to five layers of rGO encapsulating TiO_2. The composites acted as better photocatalysts for the photodegradation of Methyl orange.

1.6.3 TiO_2 modified by conjugated polymers

The idea of coupling a metal oxide photocatalyst with a polymer system was introduced in order to develop a system that could support the metal oxide for better activity. Such an immobilized system with polymer supported inorganic photocatalysts find its application in water purification systems. Polymer supported inorganic heterogeneous photocatalyst particles eliminate the troubles faced while retracting the catalyst from water after the reaction. In other words the highly dispersed catalyst particles require more time to settle after purification process and this drawback is nullified by polymer support. Based on this idea numerous polymer supports[296] were introduced, with PE being the first reported polymer for TiO_2 support[297].

The most remarkable advantage in photocatalysis was achieved with the introduction of conducting polymers having extended conjugation such as polyaniline (PANI)[298], polythiophene (PTh)[299], poly(3,4-ethylenedioxythiophene) (PEDOT)[300], Poly(3-hexylthiophene) (P3HT)[301], polypyrrole (PPy)[302], poly-(fluorene-co-thiophene) (PFT)[303] etc. These conducting conjugated polymers act as co-catalyst to enhance the activity of the photocatalyst associated with them[304]. Conducting polymers that have extended π-conjugation are quiet stable and can also absorb in UV and visible region (190 to 800 nm)[305]. The introduction of such conjugated systems coupled with photocatalysts like TiO_2 can hence extend their activity in the visible region [306].

PANI offers a better choice of conjugated conducting polymers that could be coupled with TiO_2 like photocatalysts. The characteristic property of PANI includes high charge carrier mobility along the matrix, better absorption in visible region, environmental stability and easy synthetic approach making the material cheap. PANI is a hole transporting polymer[307]. PANI can be considered as p-type material that forms p-n heterojunction with n-type TiO_2 semiconductor that further enhances the charge carrier mobility[308].

Wang et al (2007)[305] reported the preparation of TiO_2-PANI nano composite via chemical oxidative polymerisation of aniline. The prepared composite catalysed the photodegradation of Methylene blue dye, utilizing UV as well as visible region of natural light. Pure TiO_2 photocatalyst on the other hand was active only in the UV region. Min et al (2007)[309] reported the existence of coordination bond between titanium atom of TiO_2 and nitrogen atom of PANI, prepared through oxidative polymerisation method. The composite catalysed enhanced degradation of methylene blue dye under natural light compared to pure TiO_2 catalyst. Zhang and co-workers (2008)[306] reported that the improved photocatalytic activity of the synthesised TiO_2-PANI composite for the photodegradation of Methylene blue and Rhodamine B under visible light was facilitated by the $\pi \rightarrow \pi^*$ transition in PANI. The $\pi \rightarrow \pi^*$ transition caused transportation of electrons from PANI to the CB of TiO_2 and further to the adsorbed molecules (O_2 and H_2O/-OH) producing radical species. These species initiated the degradation mechanism of the dyes. Wang and co-workers (2010)[310] prepared PANI doped with camphorsulfonic acid (CSA) by dispersion polymerisation method. Composite of TiO_2-PANI-CSA was developed by dissolving PANI-CSA in THF. The photodegradation of methylene blue was studied using TiO_2 and TiO_2-PANI-CSA photocatalysts. It was concluded that PANI-CSA extended the activity of TiO_2 towards visible region of the spectra. Olad (2011)[311] developed core shell structures of TiO_2-PANI composite with PANI encapsulating TiO_2. The composite showed improved activity for the photodegradation of Methyl orange under visible light radiation. Reddy et al. (2016)[298] prepared TiO_2-PANI through oxidative polymerisation and reported that the composite showed improved photocatalytic activity under UV radiation for the photodegradation of Rhodamine B, Methylene Blue and phenol. The extent of photodegradation of Reactive red (azo dye) from waste water under UV radiation was greater in the presence of TiO_2-PANI compared to pristine TiO_2 as reported by Gilja (2017)[312].

1.7 Organic compounds as photosensitizers

Some simple organic compounds have the ability to absorb electromagnetic radiations, get excited and dissipate their energy by transferring it into another system without quenching. Such compounds come under the category of photosensitizers. Photosensitizers transfer its triplet energy into the reactant compounds coupled with

them. The use of photosensitizers hence finds their application when the triplet state yield of a particular compound is not satisfactory. In addition to triplet energy transfer, photosensitizers also involve in photocatalysis in some cases[313]. The efficiency of a molecule to act as an efficient photosensitizer depends upon the efficiency of its inter system crossing (ISC) which determines its triplet state production[314,315]. Based on the triplet state energy transfer efficiency, the choice of photosensitizers spread to a wide variety including organic compounds, organic dyes, organo-metallic compounds, transition metallic complexes etc. The application of photosensitizers is also extended to therapy, disinfection, hydrogen production, environmental remediation, luminescent oxygen sensing[316,317] and other photochemical reactions[318,319]. In polymer degradation chemistry, the photosensitisers work by producing free radicals that interacts with the polymer chains initiating photodegradation[320]. The region of light absorption and thereby the photo-reactivity/degradation of a polymer could be tuned by coupling it with suitable photosensitizer[321].

Eltayeb and co-workers (2009)[83] investigated the photodegradation of LDPE using 2-hydroxy-4-methoxybenzophenone and cobalt naphthenate photosensitizers, under UV radiation. It was observed that the rate of photodegradation of LDPE increased in the presence of cobalt naphthenate. 2-hydroxy-4-methoxybenzophenone on the other hand showed retardation in photo-oxidative degradation. In 2011 Eltayeb et al.[82] again compared the degradation of LDPE using cobalt naphthenate and 2-benzoylbenzoic acid under UV radiation. Even though the rate of photodegradation of LDPE increased as the percentage of cobalt naphthenate increased, the increase in the concentration of 2-benzoylbenzoic acid retarded the photodegradation. Manangan et al. (2010)[320] investigated the photodegradation of PE and PP using derivatives of benzophenone and acetophenone. Two different light sources (λ= 254 nm and 366 nm) were used. The photodegradation was efficient under 254 nm UV radiation. 3-nitroacetophenone showed better photosensitization for the effective degradation of PE and PP compared to the others. Pinto et al. (2013)[322] investigated the photodegradation of PS film in the presence of organic photosensitizers, thioxanthone and benzophenone. Both the photosensitizers caused oxidative degradation with the formation of double bonds in the PS chain. The photosensitization of thioxanthone was found to be superior compared to that of benzophenone. Flash photolysis proved

that both the photosensitizers exhibited same triplet state reactivity. The larger absorptivity of thioxanthone compared to benzophenone was the reason behind its superior photosensitizing efficiency. Nguyen et al. (2018)[80] developed a hybrid photocatalyst TiO_2-benzophenone-ethylene vinyl acetate by mixing process. Photodegradation of LDPE film was studied using this catalyst. The catalyst showed improved efficiency for the photodegradation of LDPE with increasing carbonyl index and decrease in the mechanical property with respect to degradation time.

1.8 Zinc oxide (ZnO)

Zinc oxide (ZnO) is a transition metal semiconductor whose photochemistry resembles that of TiO_2 in several aspects[323]. The band gap energy (E_g) of ZnO is almost equal to TiO_2 (generally E_g of ZnO is slightly greater than that of TiO_2)[324]. ZnO is also non-toxic, cheap and efficient photocatalyst just like TiO_2[325]. It is an n-type semiconductor like TiO_2[326]. ZnO has also been widely used in many applications[327,328]. Disadvantages like faster charge recombination and inactivity towards visible region is also observed in ZnO. Another disadvantage is that the photostability of ZnO is not as much pronounced as TiO_2. ZnO undergoes photo-corrosion to form $Zn(OH)_2$ when exposed to UV radiation for a prolonged time interval[329]. ZnO is also soluble in strong acidic and strong alkaline medium[329,330]. This limits the use of ZnO compared to TiO_2 in most of the cases. Some authors reported that ZnO is less efficient compared to TiO_2 as a photocatalyst. Several modification strategies have been practiced in order to increase the photocatalytic efficiency of ZnO[331–333] as explained in the case of TiO_2 in previous sections. ZnO commonly exists in zinc blende and wurtzite phases. Wurtzite phase is mostly used as photocatalysts especially in environmental cleaning processes[334,335].

Out of several studies reported using ZnO initiated photochemical reactions, recent ones include the work of Denisyuk et al. (2016)[336] who studied the photodegradation of p-type semiconductor doped acrylic polymer film. The photodegradation of the polymer was explained by the development of bubbles due to the formation of various photolysis products. Suryavanshi et al. (2018)[337] adopted spray pyrolysis method for the deposition of ZnO films over glass substrates. The photodegradation of methyl blue and benzoic acid dye were studied using these ZnO coated electrodes. Methyl blue underwent better photodegradation. Zhang et al.

(2018)[338] dried ZnO particles in vacuum in order to develop nano ZnO particles with oxygen vacancies. Photodegradation of methylene blue was studied using this nano ZnO as catalyst under UV radiation. Superior photocatalytic efficiency exhibited by the synthesised nano ZnO was reported to be due to the reduction of electron hole recombination by the oxygen vacancies, increased surface area and better photostability.

Application of ZnO catalyst modified by several techniques was also reported. Some of the recent works include the study of Ngaloy et al. (2019)[339] where chemical vapour decomposition method was used for the preparation of ZnO-rGO photocatalyst that showed improved activity for the degradation of methylene blue under UV radiation. The formation of Zn-O-C bond between ZnO and rGO improved the separation of charge carriers generated within ZnO and hence better photocatalytic activity. Asgar et al. (2019)[340] developed ZnO-PANI photocatalyst via chemical oxidative polymerisation method for the study of degradation of metronidazole under UV radiation. The photodegradation of metronidazole was accelerated by ZnO-PANI photocatalyst by the formation of highly reactive $O_2^{\bullet-}$ and $OH^{\bullet}$ radicals which interacted with metronidazole. Qi and co-workers (2019) [341] modified ZnO by doping it with some transition metals Fe, Ni, Co, Mn and Cu. The transition metal doped ZnO existed in wurtzite phase. The metal doping was 3% versus ZnO. Cu doped ZnO showed superior photocatalytic activity for the degradation of methylene blue under light radiation (λ=365 nm). Ismael et al. (2019)[342] developed ZnO modified with graphitic carbon nitride via calcination method. The composite efficiently catalysed the photodegradation of 4-chlorophenol and methyl orange in the presence of visible light. The improved degradation efficiency of the composite attributed to the easy charge transfer through the interface between the heterojunctions of the composite. Neelgud and Oki (2020)[343] developed graphene nanosheets deposited by ZnO nanotrapezoids. The composite exhibited better photostability and improved efficiency for the photodegradation of different types of dye contaminants in sunlight. The mechanism of enhancement of photocatalytic activity is due to the formation of heterojunctions formed between ZnO and graphene nanosheets that facilitated better charge transfer and reduced the charge carrier recombination.

1.9 Objectives of the present study

1. To prepare and characterise modified TiO_2/ZnO photocatalysts.
2. To study the photodegradation of PS in the presence of these photocatalysts and other photosensitizers under UV radiation.
3. To investigate the change in electrical, mechanical and thermal properties of PS-composites due to photodegradation.
4. To propose a suitable mechanism for photodegradation of PS composites.
5. To optimise the degradation conditions of PS under UV radiation.

References

1. Hosler, D., Burkett, S. L. & Tarkanian, M. J. Prehistoric Polymers: Rubber Processing in Ancient Mesoamerica. *Science (80-.).* **284**, 1988–1991 (1999).
2. Andrady, A. L. & Neal, M. A. Applications and societal benefits of plastics. *Philos. Trans. R. Soc. B Biol. Sci.* **364**, 1977–1984 (2009).
3. Staudinger, H. Über Polymerisation. *Berichte der Dtsch. Chem. Gesellschaft (A B Ser.* **53**, 1073–1085 (1920).
4. Mulder, K. F. Sustainable Consumption and Production of Plastics? *Technol. Forecast. Soc. Change* **58**, 105–124 (1998).
5. Geyer, R., Jambeck, J. R. & Law, K. L. Production, use, and fate of all plastics ever made. *Sci. Adv.* **3**, (2017).
6. Rabie, S., Mahran, A., M Kamel, E. & H Abdel Hamid, N. Photodegradation of Polystyrene Stabilized with Uracil Derivatives. *J. Appl. Sci. Res.* **4**, 2018–2026 (2008).
7. Chaukura, N., Gwenzi, W., Bunhu, T., Ruziwa, D. T. & Pumure, I. Potential uses and value-added products derived from waste polystyrene in developing countries: A review. *Resour. Conserv. Recycl.* **107**, 157–165 (2016).
8. Hocking, M. B. Paper versus polystyrene: a complex choice. *Science (80-.).* **251**, 504 (1991).
9. Priddy, D. Styrene Polymers. in *Encyclopedia of Polymer Science and Technology* 241–336 (American Cancer Society, 2001). doi:10.1002/0471440264.pst354.
10. Pasztor, A. J., Landes, B. G. & Karjala, P. J. Thermal properties of syndiotactic polystyrene. *Thermochim. Acta* **177**, 187–195 (1991).
11. Ishihara, N., Seimiya, T., Kuramoto, M. & Uoi, M. Crystalline syndiotactic polystyrene. *Macromolecules* **19**, 2464–2465 (1986).
12. Natta, G. *et al.* Crystalline High Polymers of α-olefins. *J. Am. Chem. Soc.* **77**, 1708–1710 (1955).
13. Brownstein, S., Bywater, S. & Worsfold, D. J. Proton Resonance Spectra and Tacticity of Polystyrene and Deuteriopolystyrenes. *J. Phys. Chem.* **66**, 2067–2068 (1962).
14. Bovey, F. A., Hood, F. P., Anderson, E. W. & Snyder, L. C. Polymer NMR Spectroscopy. XI. Polystyrene and Polystyrene Model Compounds. *J. Chem. Phys.* **42**, 3900–3910 (1965).
15. Heatley, F. & Bovey, F. A. Polymer Nuclear Magnetic Resonance Spectroscopy. XIII. Polystyrene at 220 MHz. *Macromolecules* **1**, 301–303 (1968).
16. Matsuzaki, K., Uryu, T., Osada, K. & Kawamura, T. Stereoregularity of polystyrene-β,β-d2. *J. Polym. Sci. Polym. Chem. Ed.* **12**, 2873–2879 (1974).
17. Tadokoro, H., Nishiyama, Y., Nozakura, S. & Murahashi, S. Stereoregular Polymers. VII. Infrared Spectra of Isotactic Polystyrene, Isotactic Poly-α, β, β-trideuterostyrene and Isotactic Poly-p- deuterostyrene. *Bull. Chem. Soc. Jpn.* **34**, 381–391 (1961).
18. Trumbo, D. L., Chen, T. K. & Harwood, H. J. Observation of triad stereosequences in a

polystyrene derivative. *Macromolecules* **14**, 1138–1139 (1981).
19. Ray, G. J., Pauls, R. E., Lewis, J. J. & Rogers, L. B. Structure determination by two-dimensional NMR of α-hydro-ω-butyloligostyrenes fractionated by liquid chromatography. *Die Makromol. Chemie* **186**, 1135–1149 (1985).
20. Johnson, L. F., Heatley, F. & Bovey, F. A. Polymer Nuclear Magnetic Resonance Spectroscopy. XIX. Carbon-13 Resonance Observations of Stereochemical Configuration. *Macromolecules* **3**, 175–177 (1970).
21. Randall, J. C. The distribution of stereochemical configurations in polystyrene as observed with 13C NMR. *J. Polym. Sci. Polym. Phys. Ed.* **13**, 889–899 (1975).
22. Cheng, H. N. & Lee, G. H. NMR Studies of Polystyrene Tacticity. *Int. J. Polym. Anal. Charact.* **2**, 439–455 (1996).
23. Tan, H., Moet, A., Hiltner, A. & Baer, E. Thermoreversible gelation of atactic polystyrene solutions. *Macromolecules* **16**, 28–34 (1983).
24. Clark, J. C., Wellinghoff, S. T. & Miller, W. G. Rheological Properties of Polystyrene Carbon-Disulfide Gels. in *Abstracts of Papers of the American Chemical Society* vol. 186 41--POLY (1983).
25. Gan, Y.-S., François, J., Guenet, J.-M., Gauthier-Manuel, B. & Allain, C. A direct demonstration of the occurrence of physical gelation in atactic polystyrene solutions. *Die Makromol. Chemie, Rapid Commun.* **6**, 225–230 (1985).
26. Gan, J. Y. S., Francois, J. & Guenet, J. M. Enhanced low-angle scattering from moderately concentrated solutions of atactic polystyrene and its relation to physical gelation. *Macromolecules* **19**, 173–178 (1986).
27. François, J., Gan, J., Sarazin, D. & Guenet, J.-M. Relation between physical gelation and tacticity in polystyrene. *Polymer (Guildf).* **29**, 898–903 (1988).
28. David, C., Putman-de Lavareille, N. & Geuskens, G. Luminescence studies in polymers—IV. Effect of orientation, tacticity and crystallinity on polystyrene and polyvinylcarbazole fluorescence. *Eur. Polym. J.* **10**, 617–621 (1974).
29. Chen, K., Harris, K. & Vyazovkin, S. Tacticity as a Factor Contributing to the Thermal Stability of Polystyrene. *Macromol. Chem. Phys.* **208**, 2525–2532 (2007).
30. Huang, C.-L., Chen, Y.-C., Hsiao, T.-J., Tsai, J.-C. & Wang, C. Effect of Tacticity on Viscoelastic Properties of Polystyrene. *Macromolecules* **44**, 6155–6161 (2011).
31. Grigoriadi, K. *et al.* Physical Ageing of Polystyrene: Does Tacticity Play a Role? *Macromolecules* **52**, 5948–5954 (2019).
32. Terashima, T. Polystyrene (PSt). in *Encyclopedia of Polymeric Nanomaterials* (eds. Kobayashi, S. & Müllen, K.) 2077–2091 (Springer Berlin Heidelberg, 2015). doi:10.1007/978-3-642-29648-2_255.
33. Priddy, D. B. Recent advances in styrene polymerization. in *Polymer Synthesis* 67–114 (Springer Berlin Heidelberg, 1994). doi:10.1007/BFb0024127.
34. Flory, P. J. The Mechanism of Vinyl Polymerizations1. *J. Am. Chem. Soc.* **59**, 241–253 (1937).
35. Mayo, F. R. The dimerization of styrene. *J. Am. Chem. Soc.* **90**, 1289–1295 (1968).
36. Mulzer, J., Kühl, U., Huttner, G. & Evertz, K. Facial selectivities and rate effects in the thermal [4+2] dimerization of arylated 1,3-dienes. 1,5-H shift versus dimerization of (Z)-1,3-Dienes. *Chem. Ber.* **121**, 2231–2238 (1988).
37. Gibbs, B. F. & Mulligan, C. N. Styrene Toxicity: An Ecotoxicological Assessment. *Ecotoxicol. Environ. Saf.* **38**, 181–194 (1997).
38. Kwon, B. G. *et al.* Regional distribution of styrene analogues generated from polystyrene degradation along the coastlines of the North-East Pacific Ocean and Hawaii. *Environ. Pollut.* **188**, 45–49 (2014).
39. LI, W. C., TSE, H. F. & FOK, L. Plastic waste in the marine environment: A review of sources, occurrence and effects. *Sci. Total Environ.* **566–567**, 333–349 (2016).
40. Singh, B. & Sharma, N. Mechanistic implications of plastic degradation. *Polym Degrad Stab* **93**, (2008).
41. Xiao, L. *et al.* Synthesis of novel ultraviolet stabilizers based on [60]fullerene and their

effects on photo-oxidative degradation of polystyrene. *Fullerenes, Nanotub. Carbon Nanostructures* **28**, 465–473 (2020).
42. Al-Khazraji, A. M. A., Hassani, R. A. M. Al & Ahmed, A. Studies on the Photostability of Polystyrene Films with New Metals Complex of 1, 2, 4-triazole-3-thione Derivate. *Syst. Rev. Pharm.* **11**, 525–534 (2020).
43. Alotaibi, M. H. *et al.* Evaluation of the use of polyphosphates as photostabilizers and in the formation of ball-like polystyrene materials. *J. Polym. Res.* **26**, 161 (2019).
44. Hadi, A. G. *et al.* Photostabilization of Poly(vinyl chloride) by Organotin(IV) Compounds against Photodegradation. *Molecules* **24**, (2019).
45. Ali, G. Q. *et al.* Photostability and Performance of Polystyrene Films Containing 1,2,4-Triazole-3-thiol Ring System Schiff Bases. *Molecules* **21**, (2016).
46. Kwon, B. G., Chung, S.-Y., Park, S.-S. & Saido, K. Qualitative assessment to determine internal and external factors influencing the origin of styrene oligomers pollution by polystyrene plastic in coastal marine environments. *Environ. Pollut.* **234**, 167–173 (2018).
47. Barnes, D. K. A., Galgani, F., Thompson, R. C. & Barlaz, M. Accumulation and fragmentation of plastic debris in global environments. *Philos. Trans. R. Soc. B Biol. Sci.* **364**, 1985–1998 (2009).
48. Cole, M., Lindeque, P., Halsband, C. & Galloway, T. S. Microplastics as contaminants in the marine environment: a review. *Mar. Pollut. Bull.* **62**, 2588–2597 (2011).
49. Eriksen, M. *et al.* Plastic pollution in the South Pacific subtropical gyre. *Mar. Pollut. Bull.* **68**, 71–76 (2013).
50. Bergami, E. *et al.* Nano-sized polystyrene affects feeding, behavior and physiology of brine shrimp Artemia franciscana larvae. *Ecotoxicol. Environ. Saf.* **123**, 18–25 (2016).
51. Barboza, L. G. A. & Gimenez, B. C. G. Microplastics in the marine environment: Current trends and future perspectives. *Mar. Pollut. Bull.* **97**, 5–12 (2015).
52. de Stephanis, R., Giménez, J., Carpinelli, E., Gutierrez-Exposito, C. & Cañadas, A. As main meal for sperm whales: plastics debris. *Mar. Pollut. Bull.* **69**, 206–214 (2013).
53. Hidalgo-Ruz, V., Gutow, L., Thompson, R. C. & Thiel, M. Microplastics in the marine environment: a review of the methods used for identification and quantification. *Environ. Sci. Technol.* **46**, 3060–3075 (2012).
54. Koelmans, A. A., Besseling, E., Wegner, A. & Foekema, E. M. Plastic as a carrier of POPs to aquatic organisms: a model analysis. *Environ. Sci. Technol.* **47**, 7812–7820 (2013).
55. Koelmans, A. A., Besseling, E. & Foekema, E. M. Leaching of plastic additives to marine organisms. *Environ. Pollut.* **187**, 49–54 (2014).
56. Thompson, R. C. *et al.* Lost at Sea: Where Is All the Plastic? *Science (80-.).* **304**, 838 (2004).
57. Chae, Y. & An, Y.-J. Current research trends on plastic pollution and ecological impacts on the soil ecosystem: A review. *Environ. Pollut.* **240**, 387–395 (2018).
58. Nizzetto, L., Bussi, G., Futter, M. N., Butterfield, D. & Whitehead, P. G. A theoretical assessment of microplastic transport in river catchments and their retention by soils and river sediments. *Environ. Sci. Process. Impacts* **18**, 1050–1059 (2016).
59. Rillig, M. C. Microplastic in terrestrial ecosystems and the soil? *Environ. Sci. Technol.* **46**, 6453–6454 (2012).
60. Liu, E. K., He, W. Q. & Yan, C. R. `White revolution' to `white pollution'{\textemdash}agricultural plastic film mulch in China. *Environ. Res. Lett.* **9**, 91001 (2014).
61. Rochman, C. M. *et al.* Scientific Evidence Supports a Ban on Microbeads. *Environ. Sci. Technol.* **49**, 10759–10761 (2015).
62. Akhtar, S. Food Safety Challenges—A Pakistan's Perspective. *Crit. Rev. Food Sci. Nutr.* **55**, 219–226 (2015).
63. Morikawa, T. & Yanai, E. Toxic Gases and Smoke Evolution from Foam Plastic Building Materials Burning in Fire Environments. *J. Fire Sci.* **7**, 131–141 (1989).

64. Gao, X., Ji, B., Yan, D., Huang, Q. & Zhu, X. A full-scale study on thermal degradation of polychlorinated dibenzo- p-dioxins and dibenzofurans in municipal solid waste incinerator fly ash and its secondary air pollution control in China. *Waste Manag. Res. J. Int. Solid Wastes Public Clean. Assoc. ISWA* **35**, 437–443 (2017).
65. Ji, L. *et al.* Municipal solid waste incineration in China and the issue of acidification: A review. *Waste Manag. Res. J. Int. Solid Wastes Public Clean. Assoc. ISWA* **34**, 280–297 (2016).
66. Ragaert, K., Delva, L. & Van Geem, K. Mechanical and chemical recycling of solid plastic waste. *Waste Manag.* **69**, 24–58 (2017).
67. Guaita, M., Chiantore, O. & Costa, L. Changes in degree of polymerization in the thermal degradation of polystyrene. *Polym. Degrad. Stab.* **12**, (1985).
68. Weidner, S., Kühn, G., Friedrich, J. & Schröder, H. Plasmaoxidative and Chemical Degradation of Poly(ethylene terephthalate) Studied by Matrix-assisted Laser Desorption/Ionization Mass Spectrometry. *Rapid Commun. Mass Spectrom.* **10**, 40–46 (1996).
69. Vinhas, G. M., Souto-Maior, R. M., Lapa, C. M. & Almeida, Y. M. B. de. Degradation studies on plasticized PVC films submited to gamma radiation. *Mater. Res.* **6**, 497–500 (2003).
70. Fotopoulou, K. N. & Karapanagioti, H. K. Degradation of Various Plastics in the Environment. in *Hazardous Chemicals Associated with Plastics in the Marine Environment* (eds. Takada, H. & Karapanagioti, H. K.) 71–92 (Springer International Publishing, 2019). doi:10.1007/698_2017_11.
71. Yousif, E. & Haddad, R. Photodegradation and photostabilization of polymers, especially polystyrene: review. *Springerplus* **2**, 398 (2013).
72. Matheson, L. A. & Boyer, R. F. Light Stability of Polystyrene and Polyvinylidene Chloride. *Ind. Eng. Chem.* **44**, 867–874 (1952).
73. Grassie, N. & Weir, N. A. The photooxidation of polymers. IV. A note on the coloration of polystyrene. *J. Appl. Polym. Sci.* **9**, 999–1003 (1965).
74. George, G. A. The phosphorescence spectrum and photodegradation of polystyrene films. *J. Appl. Polym. Sci.* **18**, 419–426 (1974).
75. Torikai, A., Takeuchi, A. & Fueki, K. The effect of temperature on the photo-degradation of polystyrene. *Polym. Degrad. Stab.* **14**, 367–375 (1986).
76. Hwang, D., Shul, Y. & Chu, Y. Photodegradation behavior of the polycarbonate/TiO2 composite films under the UV irradiation in ambient air condition. *Polym. Compos.* **36**, 1462–1468 (2014).
77. Zhao, X. u, Li, Z., Chen, Y., Shi, L. & Zhu, Y. Solid-phase photocatalytic degradation of polyethylene plastic under UV and solar light irradiation. *J. Mol. Catal. A Chem.* **268**, 101–106 (2007).
78. Al Safi, S. A., Al Mouamin, T. M., Al Sieadi, W. N. & Al Ani, K. E. Irradiation Effect on Photodegradation of Pure and Plasticized Poly (4-Methylstyrene) in Solid Films. *Mater. Sci. Appl.* **5**, 300 (2014).
79. Shawaphun, S., Sangsansiri, D., Changcharoen, J. & Wacharawichanant, S. Nano-Sized Titanium Dioxides as Photo-Catalysts in Degradation of Polyethylene and Polypropylene Packagings. *Sci. J. Ubon Ratchathani Univ.* **1**, (2010).
80. Nguyen, T. K. N. *et al.* Titanium dioxide-benzophenone hybrid as an effective catalyst for enhanced photochemical degradation of low density polyethylene. *e-Polymers* **18**, (2018).
81. Amin, M. U. & Scott, G. Photo-initiated oxidation of polyethylene effect of photo-sensitizers. *Eur. Polym. J.* **10**, 1019–1028 (1974).
82. Eltayeb, E. A., Mahdavian, A. R. & Barikani, M. The Effect of Cobalt Naphthenate and 2-benzoylbenzoic Acid on UV-Degradation Of LDPE. *Iran. J. Chem. Eng.* **8**, 31–42 (2011).
83. Eltayeb, E., Barikani, M., Mahdavian, A. R. & Honarkar, H. The Effect of Cobalt Naphthenate and 2-Hydroxy-4-Methoxybenzophenone on Photo-oxidative Degradation

of LDPE. *Iran. Polym. J.* **18**, 753–760 (2009).
84. Barboiu, V. & Avadanei, M. I. Chemical reactions of benzophenone photoirradiated in 1,2-polybutadiene. *J. Photochem. Photobiol. A Chem.* **222**, 170–179 (2011).
85. Asghar, W. *et al.* Comparative Solid Phase Photocatalytic Degradation of Polythene Films with Doped and Undoped TiO 2 Nanoparticles. **2011**, (2011).
86. Shanti, R. *et al.* Degradation of ultra-high molecular weight poly(methyl methacrylate-co-butyl acrylate-co-acrylic acid) under ultra violet irradiation. *RSC Adv.* **v. 7**, 112-120–2016 v.7 no.1 (2016).
87. Oil and Colour Chemists' Association, A. Titanium Dioxide Pigments. in *Surface Coatings: Vol I-Raw Materials and Their Usage* 305–312 (Springer Netherlands, 1983). doi:10.1007/978-94-011-6940-0_26.
88. Renz, C. Lichtreaktionen der Oxyde des Titans, Cers und der Erdsäuren. *Helv. Chim. Acta* **4**, 961–968 (1921).
89. Goodeve, C. F. & Kitchener, J. A. The mechanism of photosensitisation by solids. *Trans. Faraday Soc.* **34**, 902–908 (1938).
90. FUJISHIMA, A. & HONDA, K. Electrochemical Photolysis of Water at a Semiconductor Electrode. *Nature* **238**, 37–38 (1972).
91. Bickley, R. I., Gonzalez-Carreno, T., Lees, J. S., Palmisano, L. & Tilley, R. J. D. A structural investigation of titanium dioxide photocatalysts. *J. Solid State Chem.* **92**, 178–190 (1991).
92. Luttrell, T. *et al.* Why is anatase a better photocatalyst than rutile? - Model studies on epitaxial TiO2 films. *Sci. Rep.* **4**, 4043 (2014).
93. Latroche, M., Brohan, L., Marchand, R. & Tournoux, M. New hollandite oxides: TiO2(H) and K0.06TiO2. *J. Solid State Chem.* **81**, 78–82 (1989).
94. Marchand, R., Brohan, L. & Tournoux, M. TiO2(B) a new form of titanium dioxide and the potassium octatitanate K2Ti8O17. *Mater. Res. Bull.* **15**, 1129–1133 (1980).
95. Akimoto, J. *et al.* Topotactic Oxidation of Ramsdellite-Type Li0.5TiO2, a New Polymorph of Titanium Dioxide: TiO2(R). *J. Solid State Chem.* **113**, 27–36 (1994).
96. Mattesini, M. *et al.* High-pressure and high-temperature synthesis of the cubic TiO2 polymorph. *Phys. Rev. B* **70**, 212101 (2004).
97. Simons, P. Y. & Dachille, F. The structure of TiO2II, a high-pressure phase of TiO2. *Acta Crystallogr.* **23**, 334–336 (1967).
98. Dubrovinskaia, N. A. *et al.* Experimental and Theoretical Identification of a New High-Pressure TiO2 Polymorph. *Phys. Rev. Lett.* **87**, 275501 (2001).
99. Dubrovinsky, L. S. *et al.* The hardest known oxide. *Nature* **410**, 653–654 (2001).
100. Sato, H. *et al.* Baddeleyite-Type High-Pressure Phase of TiO2. *Science (80-.).* **251**, 786–788 (1991).
101. Tian, M. *et al.* Recent progress in characterization of the core–shell structure of black titania. *J. Mater. Res.* 1–16 (2019) doi:10.1557/jmr.2019.46.
102. Stoyanov, E., Langenhorst, F. & Steinle-Neumann, G. The effect of valence state and site geometry on Ti L 3, 2 and OK electron energy-loss spectra of TixOy phases. *Am. Mineral.* **92**, 577–586 (2007).
103. Bessekhouad, Y., Robert, D. & Weber, J. V. Synthesis of photocatalytic TiO2 nanoparticles: optimization of the preparation conditions. *J. Photochem. Photobiol. A Chem.* **157**, 47–53 (2003).
104. Oskam, G., Nellore, A., Penn, R. L. & Searson, P. C. The Growth Kinetics of TiO2 Nanoparticles from Titanium(IV) Alkoxide at High Water/Titanium Ratio. *J. Phys. Chem. B* **107**, 1734–1738 (2003).
105. Sugimoto, T. Preparation of monodispersed colloidal particles. *Adv. Colloid Interface Sci.* **28**, 65–108 (1987).
106. Anderson, M. A., Gieselmann, M. J. & Xu, Q. Titania and alumina ceramic membranes. *J. Memb. Sci.* **39**, 243–258 (1988).
107. Barringer, E. A. & Bowen, H. K. High-purity, monodisperse TiO2 powders by hydrolysis of titanium tetratethoxide. 2. Aqueous interfacial electrochemistry and

dispersion stability. *Langmuir* **1**, 420–428 (1985).
108. Kormann, C., Bahnemann, D. W. & Hoffmann, M. R. Preparation and characterization of quantum-size titanium dioxide. *J. Phys. Chem.* **92**, 5196–5201 (1988).
109. Sugimoto, T., Zhou, X. & Muramatsu, A. Synthesis of uniform anatase TiO2 nanoparticles by gel–sol method: 3. Formation process and size control. *J. Colloid Interface Sci.* **259**, 43–52 (2003).
110. Sugimoto, T., Zhou, X. & Muramatsu, A. Synthesis of uniform anatase TiO2 nanoparticles by gel–sol method: 4. Shape control. *J. Colloid Interface Sci.* **259**, 53–61 (2003).
111. Sugimoto, T., Zhou, X. & Muramatsu, A. Synthesis of Uniform Anatase TiO2 Nanoparticles by Gel–Sol Method: 1. Solution Chemistry of Ti(OH)n(4−n)+ Complexes. *J. Colloid Interface Sci.* **252**, 339–346 (2002).
112. Uekawa, N., Kajiwara, J., Kakegawa, K. & Sasaki, Y. Low Temperature Synthesis and Characterization of Porous Anatase TiO2 Nanoparticles. *J. Colloid Interface Sci.* **250**, 285–290 (2002).
113. Li, Y., White, T. J. & Lim, S. H. Low-temperature synthesis and microstructural control of titania nano-particles. *J. Solid State Chem.* **177**, 1372–1381 (2004).
114. Zhang, H. & Banfield, J. F. Understanding Polymorphic Phase Transformation Behavior during Growth of Nanocrystalline Aggregates: Insights from TiO2. *J. Phys. Chem. B* **104**, 3481–3487 (2000).
115. Zhang, H. & Banfield, J. F. Kinetics of Crystallization and Crystal Growth of Nanocrystalline Anatase in Nanometer-Sized Amorphous Titania. *Chem. Mater.* **14**, 4145–4154 (2002).
116. Zhang, H. & Banfield, J. F. Size Dependence of the Kinetic Rate Constant for Phase Transformation in TiO2 Nanoparticles. *Chem. Mater.* **17**, 3421–3425 (2005).
117. Zhang, H., Finnegan, M. & Banfield, J. F. Preparing Single-Phase Nanocrystalline Anatase from Amorphous Titania with Particle Sizes Tailored by Temperature. *Nano Lett.* **1**, 81–85 (2001).
118. Kim, K. Do & Kim, H. T. Synthesis of TiO2 nanoparticles by hydrolysis of TEOT and decrease of particle size using a two-stage mixed method. *Powder Technol.* **119**, 164–172 (2001).
119. Kim, K. Do & Kim, H. T. Synthesis of titanium dioxide nanoparticles using a continuous reaction method. *Colloids Surfaces A Physicochem. Eng. Asp.* **207**, 263–269 (2002).
120. Chen, Y., Crittenden, J. C., Hackney, S., Sutter, L. & Hand, D. W. Preparation of a Novel TiO2-Based p−n Junction Nanotube Photocatalyst. *Environ. Sci. Technol.* **39**, 1201–1208 (2005).
121. Lee, S., Jeon, C. & Park, Y. Fabrication of TiO2 Tubules by Template Synthesis and Hydrolysis with Water Vapor. *Chem. Mater.* **16**, 4292–4295 (2004).
122. Jung, J. H., Shimizu, T. & Shinkai, S. Self-assembling structures of steroidal derivatives in organic solvents and their sol–gel transcription into double-walled transition-metal oxide nanotubes. *J. Mater. Chem.* **15**, 3979–3986 (2005).
123. Yang, J., Mei, S. & Ferreira, J. M. F. Hydrothermal Fabrication of Rod-Like Rutile Nano-Particles. in *Advanced Materials Forum II* vol. 455 556–559 (Trans Tech Publications Ltd, 2004).
124. Yang, J., Mei, S. & Ferreira, J. M. F. In situ preparation of weakly flocculated aqueous anatase suspensions by a hydrothermal technique. *J. Colloid Interface Sci.* **260**, 82–88 (2003).
125. Chae, S. Y. *et al.* Preparation of Size-Controlled TiO2 Nanoparticles and Derivation of Optically Transparent Photocatalytic Films. *Chem. Mater.* **15**, 3326–3331 (2003).
126. Yang, J., Mei, S. & Ferreira, J. M. F. Hydrothermal synthesis of TiO2 nanopowders from tetraalkylammonium hydroxide peptized sols. *Mater. Sci. Eng. C* **15**, 183–185 (2001).
127. Yang, S. & Gao, L. Low-temperature Synthesis of Crystalline TiO2 Nanorods: Mass

Production Assisted by Surfactant. *Chem. Lett.* **34**, 964–965 (2005).
128. Zhang, Q. & Gao, L. Preparation of Oxide Nanocrystals with Tunable Morphologies by the Moderate Hydrothermal Method: Insights from Rutile TiO2. *Langmuir* **19**, 967–971 (2003).
129. Feng, X., Zhai, J. & Jiang, L. The Fabrication and Switchable Superhydrophobicity of TiO2 Nanorod Films. *Angew. Chemie Int. Ed.* **44**, 5115–5118 (2005).
130. Bavykin, D. V, Friedrich, J. M. & Walsh, F. C. Protonated Titanates and TiO2 Nanostructured Materials: Synthesis, Properties, and Applications. *Adv. Mater.* **18**, 2807–2824 (2006).
131. Miyauchi, M., Tokudome, H., Toda, Y., Kamiya, T. & Hosono, H. Electron field emission from TiO2 nanotube arrays synthesized by hydrothermal reaction. *Appl. Phys. Lett.* **89**, 43114 (2006).
132. Zhang, Y. X. *et al.* Hydrothermal synthesis and photoluminescence of TiO2 nanowires. *Chem. Phys. Lett.* **365**, 300–304 (2002).
133. Wei, M., Konishi, Y., Zhou, H., Sugihara, H. & Arakawa, H. A simple method to synthesize nanowires titanium dioxide from layered titanate particles. *Chem. Phys. Lett.* **400**, 231–234 (2004).
134. Kasuga, T., Hiramatsu, M., Hoson, A., Sekino, T. & Niihara, K. Formation of Titanium Oxide Nanotube. *Langmuir* **14**, 3160–3163 (1998).
135. Kasuga, T., Hiramatsu, M., Hoson, A., Sekino, T. & Niihara, K. Titania Nanotubes Prepared by Chemical Processing. *Adv. Mater.* **11**, 1307–1311 (1999).
136. Wen, B., Liu, C. & Liu, Y. Bamboo-Shaped Ag-Doped TiO2 Nanowires with Heterojunctions. *Inorg. Chem.* **44**, 6503–6505 (2005).
137. Yang, S. & Gao, L. Fabrication and shape-evolution of nanostructured TiO2 via a sol–solvothermal process based on benzene–water interfaces. *Mater. Chem. Phys.* **99**, 437–440 (2006).
138. Kim, C.-S., Moon, B. K., Park, J.-H., Tae Chung, S. & Son, S.-M. Synthesis of nanocrystalline TiO2 in toluene by a solvothermal route. *J. Cryst. Growth* **254**, 405–410 (2003).
139. Li, X.-L., Peng, Q., Yi, J.-X., Wang, X. & Li, Y. Near Monodisperse TiO2 Nanoparticles and Nanorods. *Chem. – A Eur. J.* **12**, 2383–2391 (2006).
140. Kim, C.-S., Moon, B. K., Park, J.-H., Choi, B.-C. & Seo, H.-J. Solvothermal synthesis of nanocrystalline TiO2 in toluene with surfactant. *J. Cryst. Growth* **257**, 309–315 (2003).
141. Wen, B.-M., Liu, C.-Y. & Liu, Y. Solvothermal synthesis of ultralong single-crystalline TiO2 nanowires. *New J. Chem.* **29**, 969–971 (2005).
142. Seifried, S., Winterer, M. & Hahn, H. Nanocrystalline Titania Films and Particles by Chemical Vapor Synthesis. *Chem. Vap. Depos.* **6**, 239–244 (2000).
143. Sung, J. *et al.* Preparation of ultrathin TiO2 coating on boron particles by thermal chemical vapor deposition and their oxidation-resistance performance. *J. Alloys Compd.* **767**, 924–931 (2018).
144. Alotaibi, A. M. *et al.* Chemical Vapor Deposition of Photocatalytically Active Pure Brookite TiO2 Thin Films. *Chem. Mater.* **30**, 1353–1361 (2018).
145. Nagasawa, H., Xu, J., Kanezashi, M. & Tsuru, T. Atmospheric-pressure plasma-enhanced chemical vapor deposition of UV-shielding TiO2 coatings on transparent plastics. *Mater. Lett.* **228**, 479–481 (2018).
146. Huang, W., Tang, X., Wang, Y., Koltypin, Y. & Gedanken, A. Selective synthesis of anatase and rutile via ultrasound irradiation. *Chem. Commun.* 1415–1416 (2000) doi:10.1039/B003349I.
147. Zhu, Y., Li, H., Koltypin, Y., Hacohen, Y. R. & Gedanken, A. Sonochemical synthesis of titania whiskers and nanotubes. *Chem. Commun.* 2616–2617 (2001) doi:10.1039/B108968B.
148. Yu, J. C., Yu, J., Ho, W. & Zhang, L. Preparation of highly photocatalytic active nano-sized TiO2 particles via ultrasonic irradiation. *Chem. Commun.* 1942–1943 (2001)

doi:10.1039/B105471F.
149. Yadav, H. M. *et al.* Preparation and characterization of copper-doped anatase TiO2 nanoparticles with visible light photocatalytic antibacterial activity. *J. Photochem. Photobiol. A Chem.* **280**, 32–38 (2014).
150. Marami, M. B., Farahmandjou, M. & Khoshnevisan, B. Sol-Gel Synthesis of Fe-Doped TiO2 Nanocrystals. *J. Electron. Mater.* **47**, 3741–3748 (2018).
151. Hassanjani-Roshan, A., Kazemzadeh, S. M., Vaezi, M. R. & Shokuhfar, A. Effect of sonication power on the sonochemical synthesis of titania nanoparticles. *J. Ceram. Process. Res.* **12**, 299–303 (2011).
152. Fujishima, A., Zhang, X. & Tryk, D. A. TiO2 photocatalysis and related surface phenomena. *Surf. Sci. Rep.* **63**, 515–582 (2008).
153. Fujishima, A., Rao, T. N. & Tryk, D. A. Titanium dioxide photocatalysis. *J. Photochem. Photobiol. C Photochem. Rev.* **1**, 1–21 (2000).
154. Ikeda, K., Sakai, H., Baba, R., Hashimoto, K. & Fujishima, A. Photocatalytic Reactions Involving Radical Chain Reactions Using Microelectrodes. *J. Phys. Chem. B* **101**, 2617–2620 (1997).
155. Kashif, N. & Ouyang, F. Parameters effect on heterogeneous photocatalysed degradation of phenol in aqueous dispersion of TiO2. *J. Environ. Sci.* **21**, 527–533 (2009).
156. lal S, D., T, S. J. & C, R. Solid-phase photodegradation of polystyrene by nano TiO2 under ultraviolet radiation. *Environ. Nanotechnology, Monit. Manag.* **12**, 100229 (2019).
157. Nakata, K. & Fujishima, A. TiO2 photocatalysis: Design and applications. *J. Photochem. Photobiol. C Photochem. Rev.* **13**, 169–189 (2012).
158. Liu, B. *et al.* Mesoporous TiO2 Core–Shell Spheres Composed of Nanocrystals with Exposed High-Energy Facets: Facile Synthesis and Formation Mechanism. *Langmuir* **27**, 8500–8508 (2011).
159. Yao, L. *et al.* Electrospinning and Stabilization of Fully Hydrolyzed Poly(Vinyl Alcohol) Fibers. *Chem. Mater.* **15**, 1860–1864 (2003).
160. Nakata, K. *et al.* Fabrication and Photocatalytic Properties of TiO2 Nanotube Arrays Modified with Phosphate. *Chem. Lett.* **40**, 1107–1109 (2011).
161. Lee, K. H., Kim, H. Y., Khil, M. S., Ra, Y. M. & Lee, D. R. Characterization of nano-structured poly(ε-caprolactone) nonwoven mats via electrospinning. *Polymer (Guildf).* **44**, 1287–1294 (2003).
162. Katsumata, K. *et al.* Preparation and Characterization of Self-Cleaning Glass for Vehicle with Niobia Nanosheets. *ACS Appl. Mater. Interfaces* **2**, 1236–1241 (2010).
163. Barakat, M. A. Adsorption and photodegradation of Procion yellow H-EXL dye in textile wastewater over TiO2 suspension. *J. Hydro-environment Res.* **5**, 137–142 (2011).
164. Zhang, T. *et al.* Photooxidative N-demethylation of methylene blue in aqueous TiO2 dispersions under UV irradiation. *J. Photochem. Photobiol. A Chem.* **140**, 163–172 (2001).
165. Gupta, V. K. *et al.* Photo-catalytic degradation of toxic dye amaranth on TiO2/UV in aqueous suspensions. *Mater. Sci. Eng. C* **32**, 12–17 (2012).
166. Faisal, M., Abu Tariq, M. & Muneer, M. Photocatalysed degradation of two selected dyes in UV-irradiated aqueous suspensions of titania. *Dye. Pigment.* **72**, 233–239 (2007).
167. Chen, J., Liu, M., Zhang, J., Ying, X. & Jin, L. Photocatalytic degradation of organic wastes by electrochemically assisted TiO2 photocatalytic system. *J. Environ. Manage.* **70**, 43–47 (2004).
168. Mahmoodi, N. M., Arami, M., Limaee, N. Y. & Tabrizi, N. S. Decolorization and aromatic ring degradation kinetics of Direct Red 80 by UV oxidation in the presence of hydrogen peroxide utilizing TiO2 as a photocatalyst. *Chem. Eng. J.* **112**, 191–196 (2005).

169. Tang, W. Z. & Huren An. UV/TiO2 photocatalytic oxidation of commercial dyes in aqueous solutions. *Chemosphere* **31**, 4157–4170 (1995).
170. Tang, C. & Chen, V. The photocatalytic degradation of reactive black 5 using TiO2/UV in an annular photoreactor. *Water Res.* **38**, 2775–2781 (2004).
171. Wu, C.-H. Effects of operational parameters on the decolorization of C.I. Reactive Red 198 in UV/TiO2-based systems. *Dye. Pigment.* **77**, 31–38 (2008).
172. Naeem, K. & Feng, O. Parameters e ff ect on heterogeneous photocatalysed degradation of phenol in aqueous dispersion of TiO 2. **21**, 527–533 (2009).
173. Liu, S., Jaffrezic, N. & Guillard, C. Size effects in liquid-phase photo-oxidation of phenol using nanometer-sized TiO2 catalysts. *Appl. Surf. Sci.* **255**, 2704–2709 (2008).
174. Górska, P. *et al.* TiO2 photoactivity in vis and UV light: The influence of calcination temperature and surface properties. *Appl. Catal. B Environ.* **84**, 440–447 (2008).
175. Ruppert, G., Bauer, R. & Heisler, G. UV-O3, UV-H2O2, UV-TiO2 and the photo-Fenton reaction - comparison of advanced oxidation processes for wastewater treatment. *Chemosphere* **28**, 1447–1454 (1994).
176. Shukla, S. S., Dorris, K. L. & Chikkaveeraiah, B. V. Photocatalytic degradation of 2,4-dinitrophenol. *J. Hazard. Mater.* **164**, 310–314 (2009).
177. Tsai, W.-T., Lee, M.-K., Su, T.-Y. & Chang, Y.-M. Photodegradation of bisphenol-A in a batch TiO2 suspension reactor. *J. Hazard. Mater.* **168**, 269–275 (2009).
178. Kaneco, S., Rahman, M. A., Suzuki, T., Katsumata, H. & Ohta, K. Optimization of solar photocatalytic degradation conditions of bisphenol A in water using titanium dioxide. *J. Photochem. Photobiol. A Chem.* **163**, 419–424 (2004).
179. Nakata, K. *et al.* Antireflection and Self-Cleaning Properties of a Moth-Eye-Like Surface Coated with TiO2 Particles. *Langmuir* **27**, 3275–3278 (2011).
180. Wang, R. *et al.* Light-induced amphiphilic surfaces. *Nature* **388**, 431–432 (1997).
181. Nakata, K. *et al.* Fabrication and Application of TiO2-Based Superhydrophilic–Superhydrophobic Patterns on Titanium Substrates for Offset Printing. *Chem. – An Asian J.* **4**, 984–988 (2009).
182. Nishimoto, S. *et al.* TiO2-based superhydrophobic–superhydrophilic patterns: Fabrication via an ink-jet technique and application in offset printing. *Appl. Surf. Sci.* **255**, 6221–6225 (2009).
183. Nakata, K. *et al.* Fabrication of micro-patterned TiO2 thin films incorporating Ag nanoparticles. *Mater. Lett.* **63**, 1628–1630 (2009).
184. Cho, S. & Choi, W. Solid-phase photocatalytic degradation of PVC–TiO2 polymer composites. *J. Photochem. Photobiol. A Chem.* **143**, 221–228 (2001).
185. Zhao, X., Li, Z., Chen, Y., Shi, L. & Zhu, Y. Enhancement of photocatalytic degradation of polyethylene plastic with CuPc modified TiO2 photocatalyst under solar light irradiation. *Appl. Surf. Sci.* **254**, 1825–1829 (2008).
186. Thomas, R. T., Nair, V. & Sandhyarani, N. TiO2 nanoparticle assisted solid phase photocatalytic degradation of polythene film: A mechanistic investigation. *Colloids Surfaces A Physicochem. Eng. Asp.* **422**, 1–9 (2013).
187. Shang, J., Chai, M. & Zhu, Y. Solid-phase photocatalytic degradation of polystyrene plastic with TiO2 as photocatalyst. *J. Solid State Chem.* **174**, 104–110 (2003).
188. Jaleh, B. *et al.* UV-degradation effect on optical and surface properties of polystyrene-TiO2 nanocomposite film. *J. Iran. Chem. Soc.* **8**, S161--S168 (2011).
189. Huang, F., Yan, A. & Zhao, H. Influences of doping on photocatalytic properties of TiO2 photocatalyst. *Semicond. Photocatal. Mech. Appl. Cao, W., Ed* 31–80 (2016).
190. Zaleska, A. Doped-TiO2: A Review. *Recent Patents Eng.* **2**, 156–164 (2008).
191. Tong, T., Zhang, J., Tian, B., Chen, F. & He, D. Preparation of Fe3+-doped TiO2 catalysts by controlled hydrolysis of titanium alkoxide and study on their photocatalytic activity for methyl orange degradation. *J. Hazard. Mater.* **155**, 572–579 (2008).
192. Xiao, J., Peng, T., Li, R., Peng, Z. & Yan, C. Preparation, phase transformation and photocatalytic activities of cerium-doped mesoporous titania nanoparticles. *J. Solid State Chem.* **179**, 1161–1170 (2006).

193. Asiltürk, M., Sayılkan, F. & Arpaç, E. Effect of Fe3+ ion doping to TiO2 on the photocatalytic degradation of Malachite Green dye under UV and vis-irradiation. *J. Photochem. Photobiol. A Chem.* **203**, 64–71 (2009).
194. Bettinelli, M. *et al.* Photocatalytic activity of TiO2 doped with boron and vanadium. *J. Hazard. Mater.* **146**, 529–534 (2007).
195. Adán, C., Carbajo, J., Bahamonde, A. & Martínez-Arias, A. Phenol photodegradation with oxygen and hydrogen peroxide over TiO2 and Fe-doped TiO2. *Catal. Today* **143**, 247–252 (2009).
196. Sakthivel, S. *et al.* Enhancement of photocatalytic activity by metal deposition: characterisation and photonic efficiency of Pt, Au and Pd deposited on TiO2 catalyst. *Water Res.* **38**, 3001–3008 (2004).
197. Kozlova, E. A. & Vorontsov, A. V. Influence of mesoporous and platinum-modified titanium dioxide preparation methods on photocatalytic activity in liquid and gas phase. *Appl. Catal. B Environ.* **77**, 35–45 (2007).
198. Sun, W., Zhang, S., Liu, Z., Wang, C. & Mao, Z. Studies on the enhanced photocatalytic hydrogen evolution over Pt/PEG-modified TiO2 photocatalysts. *Int. J. Hydrogen Energy* **33**, 1112–1117 (2008).
199. Huang, M. *et al.* Photocatalytic discolorization of methyl orange solution by Pt modified TiO2 loaded on natural zeolite. *Dye. Pigment.* **77**, 327–334 (2008).
200. Wang, C. *et al.* Preparation, characterization, photocatalytic properties of titania hollow sphere doped with cerium. *J. Hazard. Mater.* **178**, 517–521 (2010).
201. Bessekhouad, Y., Robert, D., Weber, J.-V. & Chaoui, N. Effect of alkaline-doped TiO2 on photocatalytic efficiency. *J. Photochem. Photobiol. A Chem.* **167**, 49–57 (2004).
202. Panagiotopoulou, P. & Kondarides, D. I. Effects of promotion of TiO2 with alkaline earth metals on the chemisorptive properties and water–gas shift activity of supported platinum catalysts. *Appl. Catal. B Environ.* **101**, 738–746 (2011).
203. Matsumoto, Y. Photoelectrochemical Properties of Polycrystalline TiO 2 Doped with 3d Transition Metals. *J. Electrochem. Soc.* **128**, 1040 (1981).
204. Song, K., Han, X. & Shao, G. Electronic properties of rutile TiO2 doped with 4d transition metals: First-principles study. *J. Alloys Compd.* **551**, 118–124 (2013).
205. Chen, W. *et al.* Electronic properties of anatase TiO2 doped by lanthanides: A DFT+U study. *Phys. B Condens. Matter* **407**, 1038–1043 (2012).
206. Barakat, M. A. & Kumar, R. Photocatalytic Activity Enhancement of Titanium Dioxide Nanoparticles. in *Photocatalytic Activity Enhancement of Titanium Dioxide Nanoparticles: Degradation of Pollutants in Wastewater* 1–29 (Springer International Publishing, 2016). doi:10.1007/978-3-319-24271-2_1.
207. Moma, J. & Baloyi, J. Modified titanium dioxide for photocatalytic applications. in *Photocatalysts-Applications and Attributes* (IntechOpen, 2018). doi:http://dx.doi.org/10.5772/intechopen.79374.
208. Inturi, S. N. R., Boningari, T., Suidan, M. & Smirniotis, P. G. Visible-light-induced photodegradation of gas phase acetonitrile using aerosol-made transition metal (V, Cr, Fe, Co, Mn, Mo, Ni, Cu, Y, Ce, and Zr) doped TiO2. *Appl. Catal. B Environ.* **144**, 333–342 (2014).
209. Wang, Y. *et al.* The Effects of Doping Copper and Mesoporous Structure on Photocatalytic Properties of TiO_2. *J. Nanomater.* **2014**, 178152 (2014).
210. Lin, J. C.-T., Sopajaree, K., Jitjanesuwan, T. & Lu, M.-C. Application of visible light on copper-doped titanium dioxide catalyzing degradation of chlorophenols. *Sep. Purif. Technol.* **191**, 233–243 (2018).
211. Garcidueñas-Piña, C. *et al.* Evaluation of the Antimicrobial Activity of Nanostructured Materials of Titanium Dioxide Doped with Silver and/or Copper and Their Effects on *Arabidopsis thaliana*. *Int. J. Photoenergy* **2016**, 8060847 (2016).
212. Kavitha, V., Ramesh, P. S. & Geetha, D. Synthesis of Cu Loaded TiO2 Nanoparticles for the Improved Photocatalytic Degradation of Rhodamine B. *Int. J. Nanosci.* **15**, 1660002 (2016).

213. Sahoo, C., Gupta, A. K. & Pal, A. Photocatalytic degradation of Crystal Violet (C.I. Basic Violet 3) on silver ion doped TiO2. *Dye. Pigment.* **66**, 189–196 (2005).
214. Sobana, N., Muruganadham, M. & Swaminathan, M. Nano-Ag particles doped TiO2 for efficient photodegradation of Direct azo dyes. *J. Mol. Catal. A Chem.* **258**, 124–132 (2006).
215. Sobana, N., Selvam, K. & Swaminathan, M. Optimization of photocatalytic degradation conditions of Direct Red 23 using nano-Ag doped TiO2. *Sep. Purif. Technol.* **62**, 648–653 (2008).
216. Sung-Suh, H. M., Choi, J. R., Hah, H. J., Koo, S. M. & Bae, Y. C. Comparison of Ag deposition effects on the photocatalytic activity of nanoparticulate TiO2 under visible and UV light irradiation. *J. Photochem. Photobiol. A Chem.* **163**, 37–44 (2004).
217. Behnajady, M. A., Modirshahla, N., Shokri, M. & Rad, B. Enhancement of photocatalytic activity of TiO2 nanoparticles by silver doping: photodeposition versus liquid impregnation methods. (2008).
218. Ambrus, Z. *et al.* Synthesis, structure and photocatalytic properties of Fe(III)-doped TiO2 prepared from TiCl3. *Appl. Catal. B Environ.* **81**, 27–37 (2008).
219. Mogal, S. I. *et al.* Single-Step Synthesis of Silver-Doped Titanium Dioxide : In fl uence of Silver on Structural , Textural , and Photocatalytic Properties. *Ind. Eng. Chem. Res.* **53**, 5749−5758 (2014).
220. Chiang, K., Amal, R. & Tran, T. Photocatalytic degradation of cyanide using titanium dioxide modified with copper oxide. *Adv. Environ. Res.* **6**, 471–485 (2002).
221. Wang, S., Meng, K. K., Zhao, L., Jiang, Q. & Lian, J. S. Superhydrophilic Cu-doped TiO2 thin film for solar-driven photocatalysis. *Ceram. Int.* **40**, 5107–5110 (2014).
222. Zhang, F.-S., Nriagu, J. O. & Itoh, H. Photocatalytic removal and recovery of mercury from water using TiO2-modified sewage sludge carbon. *J. Photochem. Photobiol. A Chem.* **167**, 223–228 (2004).
223. Wang, W., Silva, C. G. & Faria, J. L. Photocatalytic degradation of Chromotrope 2R using nanocrystalline TiO2/activated-carbon composite catalysts. *Appl. Catal. B Environ.* **70**, 470–478 (2007).
224. Woan, K., Pyrgiotakis, G. & Sigmund, W. Photocatalytic Carbon-Nanotube–TiO2 Composites. *Adv. Mater.* **21**, 2233–2239 (2009).
225. Yu, J., Ma, T. & Liu, S. Enhanced photocatalytic activity of mesoporous TiO2 aggregates by embedding carbon nanotubes as electron-transfer channel. *Phys. Chem. Chem. Phys.* **13**, 3491–3501 (2011).
226. Meng, Z.-D., Zhu, L., Choi, J.-G., Chen, M.-L. & Oh, W.-C. Effect of Pt treated fullerene/TiO2 on the photocatalytic degradation of MO under visible light. *J. Mater. Chem.* **21**, 7596–7603 (2011).
227. Liang, Y., Wang, H., Sanchez Casalongue, H., Chen, Z. & Dai, H. TiO2 nanocrystals grown on graphene as advanced photocatalytic hybrid materials. *Nano Res.* **3**, 701–705 (2010).
228. Liu, H. *et al.* A green and direct synthesis of graphene oxide encapsulated TiO2 core/shell structures with enhanced photoactivity. *Chem. Eng. J.* **230**, 279–285 (2013).
229. Bamba, D. *et al.* Synthesis and characterization of TiO2/C nanomaterials: Applications in water treatment. *Phys. status solidi* **252**, 2503–2511 (2015).
230. Chen, J., Qiu, F., Xu, W., Cao, S. & Zhu, H. Recent progress in enhancing photocatalytic efficiency of TiO2-based materials. *Appl. Catal. A Gen.* **495**, 131–140 (2015).
231. Nouri, E., Mohammadi, M. R. & Lianos, P. Impact of preparation method of TiO2-RGO nanocomposite photoanodes on the performance of dye-sensitized solar cells. *Electrochim. Acta* **219**, 38–48 (2016).
232. Perera, S. D. *et al.* Hydrothermal Synthesis of Graphene-TiO2 Nanotube Composites with Enhanced Photocatalytic Activity. *ACS Catal.* **2**, 949–956 (2012).
233. Kamat, P. V. Graphene-Based Nanoassemblies for Energy Conversion. *J. Phys. Chem. Lett.* **2**, 242–251 (2011).

234. Naknikham, U. *et al.* Mutual-stabilization in chemically bonded graphene oxide–TiO2 heterostructures synthesized by a sol–gel approach. *RSC Adv.* **7**, 41217–41227 (2017).
235. Zhang, H., Lv, X., Li, Y., Wang, Y. & Li, J. P25-graphene composite as a high performance photocatalyst. *ACS Nano* **4**, 380–386 (2009).
236. Khannam, M., Sharma, S., Dolui, S. & Dolui, S. K. A graphene oxide incorporated TiO2 photoanode for high efficiency quasi solid state dye sensitized solar cells based on a poly-vinyl alcohol gel electrolyte. *RSC Adv.* **6**, 55406–55414 (2016).
237. Shi, J. On the Synergetic Catalytic Effect in Heterogeneous Nanocomposite Catalysts. *Chem. Rev.* **113**, 2139–2181 (2013).
238. Li, Y., Li, X., Li, J. & Yin, J. Photocatalytic degradation of methyl orange by TiO2-coated activated carbon and kinetic study. *Water Res.* **40**, 1119–1126 (2006).
239. Mo, D. & Ye, D. Surface study of composite photocatalyst based on plasma modified activated carbon fibers with TiO2. *Surf. Coatings Technol.* **203**, 1154–1160 (2009).
240. Slimen, H., Houas, A. & Nogier, J. P. Elaboration of stable anatase TiO2 through activated carbon addition with high photocatalytic activity under visible light. *J. Photochem. Photobiol. A Chem.* **221**, 13–21 (2011).
241. Orha, C., Pode, R., Manea, F., Lazau, C. & Bandas, C. Titanium dioxide-modified activated carbon for advanced drinking water treatment. *Process Saf. Environ. Prot.* **108**, 26–33 (2017).
242. Wang, W., Serp, P., Kalck, P., Silva, C. G. & Faria, J. L. Preparation and characterization of nanostructured MWCNT-TiO2 composite materials for photocatalytic water treatment applications. *Mater. Res. Bull.* **43**, 958–967 (2008).
243. Lee, K.-Y., Yeoh, W.-M., Chai, S.-P., Ichikawa, S. & Mohamed, A. R. Optimization of Carbon Nanotubes Synthesis via Methane Decomposition over Alumina-Based Catalyst. *Fullerenes, Nanotub. Carbon Nanostructures* **18**, 273–284 (2010).
244. Yen, C.-Y. *et al.* The effects of synthesis procedures on the morphology and photocatalytic activity of multi-walled carbon nanotubes/TiO2 nanocomposites. *Nanotechnology* **19**, 45604 (2008).
245. Gao, B., Chen, G. Z. & Li Puma, G. Carbon nanotubes/titanium dioxide (CNTs/TiO2) nanocomposites prepared by conventional and novel surfactant wrapping sol–gel methods exhibiting enhanced photocatalytic activity. *Appl. Catal. B Environ.* **89**, 503–509 (2009).
246. Ashkarran, A. A., Fakhari, M., Hamidinezhad, H., Haddadi, H. & Nourani, M. R. TiO2 nanoparticles immobilized on carbon nanotubes for enhanced visible-light photo-induced activity. *J. Mater. Res. Technol.* **4**, 126–132 (2015).
247. Wongaree, M., Chiarakorn, S., Chuangchote, S. & Sagawa, T. Photocatalytic performance of electrospun CNT/TiO2 nanofibers in a simulated air purifier under visible light irradiation. *Environ. Sci. Pollut. Res.* **23**, 21395–21406 (2016).
248. Ahmad, A., Razali, M. H., Mamat, M., Mehamod, F. S. B. & Anuar Mat Amin, K. Adsorption of methyl orange by synthesized and functionalized-CNTs with 3-aminopropyltriethoxysilane loaded TiO2 nanocomposites. *Chemosphere* **168**, 474–482 (2017).
249. Scuseria, G. E. The equilibrium structure of C70. An ab initio Hartree-Fock study. *Chem. Phys. Lett.* **180**, 451–456 (1991).
250. Wang, X. *et al.* Enhanced Photocurrent Spectral Response in Low-Bandgap Polyfluorene and C70-Derivative-Based Solar Cells. *Adv. Funct. Mater.* **15**, 1665–1670 (2005).
251. He, Y. *et al.* High performance low band gap polymer solar cells with a non-conventional acceptor. *Chem. Commun.* **48**, 7616–7618 (2012).
252. Zhu, S., Xu, T., Fu, H., Zhao, J. & Zhu, Y. Synergetic Effect of Bi2WO6 Photocatalyst with C60 and Enhanced Photoactivity under Visible Irradiation. *Environ. Sci. Technol.* **41**, 6234–6239 (2007).
253. Hasobe, T., Hattori, S., Kamat, P. V & Fukuzumi, S. Supramolecular nanostructured assemblies of different types of porphyrins with fullerene using TiO2 nanoparticles for

light energy conversion. *Tetrahedron* **62**, 1937–1946 (2006).
254. Kamat, P. V, Haria, M. & Hotchandani, S. C60 Cluster as an Electron Shuttle in a Ru(II)-Polypyridyl Sensitizer-Based Photochemical Solar Cell. *J. Phys. Chem. B* **108**, 5166–5170 (2004).
255. Sibley, S. P., Argentine, S. M. & Francis, A. H. A photoluminescence study of C60 and C70. *Chem. Phys. Lett.* **188**, 187–193 (1992).
256. Lin, J., Zong, R., Zhou, M. & Zhu, Y. Photoelectric catalytic degradation of methylene blue by C60-modified TiO2 nanotube array. *Appl. Catal. B Environ.* **89**, 425–431 (2009).
257. Mu, S., Long, Y., Kang, S.-Z. & Mu, J. Surface modification of TiO2 nanoparticles with a C60 derivative and enhanced photocatalytic activity for the reduction of aqueous Cr(VI) ions. *Catal. Commun.* **11**, 741–744 (2010).
258. Long, Y. *et al.* Effect of C60 on the Photocatalytic Activity of TiO2 Nanorods. *J. Phys. Chem. C* **113**, 13899–13905 (2009).
259. Krishna, V., Noguchi, N., Koopman, B. & Moudgil, B. Enhancement of titanium dioxide photocatalysis by water-soluble fullerenes. *J. Colloid Interface Sci.* **304**, 166–171 (2006).
260. Zhang, X., Wang, Q., Zou, L.-H. & You, J.-W. Facile fabrication of titanium dioxide/fullerene nanocomposite and its enhanced visible photocatalytic activity. *J. Colloid Interface Sci.* **466**, 56–61 (2016).
261. Yu, J., Ma, T., Liu, G. & Cheng, B. Enhanced photocatalytic activity of bimodal mesoporous titania powders by C60 modification. *Dalt. Trans.* **40**, 6635–6644 (2011).
262. Qi, K. *et al.* Enhanced photocatalytic activity of anatase-TiO2 nanoparticles by fullerene modification: A theoretical and experimental study. *Appl. Surf. Sci.* **387**, 750–758 (2016).
263. Cho, E.-C. *et al.* Fullerene C70 decorated TiO2 nanowires for visible-light-responsive photocatalyst. *Appl. Surf. Sci.* **355**, 536–546 (2015).
264. Marcano, D. C. *et al.* Improved Synthesis of Graphene Oxide. *ACS Nano* **4**, 4806–4814 (2010).
265. Novoselov, K. S. *et al.* Two-dimensional gas of massless Dirac fermions in graphene. *Nature* **438**, 197–200 (2005).
266. Novoselov, K. S. *et al.* Electric Field Effect in Atomically Thin Carbon Films. *Science (80-.).* **306**, 666–669 (2004).
267. Lee, C., Wei, X., Kysar, J. W. & Hone, J. Measurement of the elastic properties and intrinsic strength of monolayer graphene. *Science (80-.).* **321**, 385–388 (2008).
268. Mohanty, N. & Berry, V. Graphene-Based Single-Bacterium Resolution Biodevice and DNA Transistor: Interfacing Graphene Derivatives with Nanoscale and Microscale Biocomponents. *Nano Lett.* **8**, 4469–4476 (2008).
269. Geim, A. K. & Novoselov, K. S. The rise of graphene. *Nat. Mater.* **6**, 183–191 (2007).
270. Balandin, A. A. *et al.* Superior Thermal Conductivity of Single-Layer Graphene. *Nano Lett.* **8**, 902–907 (2008).
271. Zhang, Y., Tang, Z.-R., Fu, X. & Xu, Y.-J. Engineering the Unique 2D Mat of Graphene to Achieve Graphene-TiO2 Nanocomposite for Photocatalytic Selective Transformation: What Advantage does Graphene Have over Its Forebear Carbon Nanotube? *ACS Nano* **5**, 7426–7435 (2011).
272. Stankovich, S. *et al.* Graphene-based composite materials. *Nature* **442**, 282–286 (2006).
273. Liu, Z., Robinson, J. T., Sun, X. & Dai, H. PEGylated Nanographene Oxide for Delivery of Water-Insoluble Cancer Drugs. *J. Am. Chem. Soc.* **130**, 10876–10877 (2008).
274. Wang, X., Zhi, L. & Müllen, K. Transparent, Conductive Graphene Electrodes for Dye-Sensitized Solar Cells. *Nano Lett.* **8**, 323–327 (2008).
275. Novoselov, K. S. *et al.* Room-Temperature Quantum Hall Effect in Graphene. *Science (80-.).* **315**, 1379 (2007).
276. Robinson, J. T., Perkins, F. K., Snow, E. S., Wei, Z. & Sheehan, P. E. Reduced

graphene oxide molecular sensors. *Nano Lett.* **8**, 3137–3140 (2008).
277. Blake, P. *et al.* Graphene-Based Liquid Crystal Device. *Nano Lett.* **8**, 1704–1708 (2008).
278. Abanin, D. A. *et al.* Dissipative Quantum Hall Effect in Graphene near the Dirac Point. *Phys. Rev. Lett.* **98**, 196806 (2007).
279. Stoller, M. D., Park, S., Zhu, Y., An, J. & Ruoff, R. S. Graphene-based ultracapacitors. *Nano Lett.* **8**, 3498–3502 (2008).
280. Wehling, T. O. *et al.* Molecular Doping of Graphene. *Nano Lett.* **8**, 173–177 (2008).
281. Sundaram, R. S., Gómez-Navarro, C., Balasubramanian, K., Burghard, M. & Kern, K. Electrochemical Modification of Graphene. *Adv. Mater.* **20**, 3050–3053 (2008).
282. Park, S. & Ruoff, R. S. Chemical methods for the production of graphenes. *Nat. Nanotechnol.* **4**, 217–224 (2009).
283. He, H., Riedl, T., Lerf, A. & Klinowski, J. Solid-State NMR Studies of the Structure of Graphite Oxide. *J. Phys. Chem.* **100**, 19954–19958 (1996).
284. He, H., Klinowski, J., Forster, M. & Lerf, A. A new structural model for graphite oxide. *Chem. Phys. Lett.* **287**, 53–56 (1998).
285. Lerf, A., He, H., Forster, M. & Klinowski, J. Structure of Graphite Oxide Revisited. *J. Phys. Chem. B* **102**, 4477–4482 (1998).
286. Cai, W. *et al.* Synthesis and Solid-State NMR Structural Characterization of 13C-Labeled Graphite Oxide. *Science (80-.).* **321**, 1815–1817 (2008).
287. Dreyer, D. R., Park, S., Bielawski, C. W. & Ruoff, R. S. The chemistry of graphene oxide. *Chem. Soc. Rev.* **39**, 228–240 (2010).
288. Kamat, P. V. Graphene-Based Nanoarchitectures. Anchoring Semiconductor and Metal Nanoparticles on a Two-Dimensional Carbon Support. 520–527 (2010) doi:10.1021/jz900265j.
289. Williams, G., Seger, B. & Kamat, P. V. TiO2-Graphene Nanocomposites. UV-Assisted Photocatalytic Reduction of Graphene Oxide. *ACS Nano* **2**, 1487–1491 (2008).
290. Hummers, W. S. & Offeman, R. E. Preparation of Graphitic Oxide. *J. Am. Chem. Soc.* **80**, 1339 (1958).
291. Kang, J. H. *et al.* Hidden Second Oxidation Step of Hummers Method. *Chem. Mater.* **28**, 756–764 (2016).
292. Huang, Q. *et al.* Enhanced Photocatalytic Activity of Chemically Bonded TiO2/Graphene Composites Based on the Effective Interfacial Charge Transfer through the C–Ti Bond. *ACS Catal.* **3**, 1477–1485 (2013).
293. Umrao, S. *et al.* A possible mechanism for the emergence of an additional band gap due to a Ti–O–C bond in the TiO2–graphene hybrid system for enhanced photodegradation of methylene blue under visible light. *RSC Adv.* **4**, 59890–59901 (2014).
294. Rakkesh, R. A., Durgalakshmi, D. & Balakumar, S. Efficient sunlight-driven photocatalytic activity of chemically bonded GNS–TiO2 and GNS–ZnO heterostructures. *J. Mater. Chem. C* **2**, 6827–6834 (2014).
295. He, D., Li, Y., Wang, J., Yang, Y. & An, and Q. Tunable Nanostructure of TiO_2/Reduced Graphene Oxide Composite for High Photocatalysis. *Appl. Microsc.* **46**, 37–44 (2016).
296. Singh, S., Mahalingam, H. & Singh, P. K. Polymer-supported titanium dioxide photocatalysts for environmental remediation: A review. *Appl. Catal. A Gen.* **462**–**463**, 178–195 (2013).
297. Tennakone, K., Tilakaratne, C. T. K. & Kottegoda, I. R. M. Photocatalytic degradation of organic contaminants in water with TiO2 supported on polythene films. *J. Photochem. Photobiol. A Chem.* **87**, 177–179 (1995).
298. Raghava, K., Karthik, K. V, Prasad, S. B. B., Soni, S. K. & Jeong, H. M. Enhanced photocatalytic activity of nanostructured titanium dioxide / polyaniline hybrid photocatalysts Enhanced photocatalytic activity of nanostructured titanium dioxide / polyaniline hybrid photocatalysts. *Polyhedron* **120**, 169–174 (2016).
299. Ansari, M. O., Khan, M. M., Ansari, S. A. & Cho, M. H. Polythiophene

nanocomposites for photodegradation applications: Past, present and future. *J. Saudi Chem. Soc.* **19**, 494–504 (2015).
300. Abdiryim, T., Ali, A., Jamal, R., Osman, Y. & Zhang, Y. A facile solid-state heating method for preparation of poly(3,4-ethelenedioxythiophene)/ZnO nanocomposite and photocatalytic activity. *Nanoscale Res. Lett.* **9**, 89 (2014).
301. Duan, Y. *et al.* An efficient visible light photocatalyst poly(3-hexylthiophene)/CdS nanocomposite with enhanced antiphotocorrosion property. *Superlattices Microstruct.* **67**, 61–71 (2014).
302. Dimitrijevic, N. M. *et al.* Nanostructured TiO2/Polypyrrole for Visible Light Photocatalysis. *J. Phys. Chem. C* **117**, 15540–15544 (2013).
303. Qiu, R. *et al.* Photocatalytic activity of polymer-modified ZnO under visible light irradiation. *J. Hazard. Mater.* **156**, 80–85 (2008).
304. Su, Y.-W., Lin, W.-H., Hsu, Y.-J. & Wei, K.-H. Conjugated Polymer/Nanocrystal Nanocomposites for Renewable Energy Applications in Photovoltaics and Photocatalysis. *Small* **10**, 4427–4442 (2014).
305. Wang, F. & Min, S. X. TiO2/polyaniline composites: An efficient photocatalyst for the degradation of methylene blue under natural light. *Chinese Chem. Lett.* **18**, 1273–1277 (2007).
306. Zhang, H., Zong, R., Zhao, J. & Zhu, Y. Dramatic Visible Photocatalytic Degradation Performances Due to Synergetic Effect of TiO2 with PANI. *Environ. Sci. Technol.* **42**, 3803–3807 (2008).
307. Zhang, H., Zong, R. & Zhu, Y. Photocorrosion Inhibition and Photoactivity Enhancement for Zinc Oxide via Hybridization with Monolayer Polyaniline. *J. Phys. Chem.* **113**, 4605–4611 (2009).
308. Ganesan, R. & Gedanken, A. Organic-organic hybrid materials based on polyaniline/TiO2 nanocomposites for ascorbic acid fuel cell systems. *Nanotechnology* **19**, 435709 (2008).
309. Min, S., Wang, F. & Han, Y. An investigation on synthesis and photocatalytic activity of polyaniline sensitized nanocrystalline TiO2 composites. *J. Mater. Sci.* **42**, 9966–9972 (2007).
310. Wang, F., Min, S., Han, Y. & Feng, L. Visible-light-induced photocatalytic degradation of methylene blue with polyaniline-sensitized TiO2 composite photocatalysts. *Superlattices Microstruct.* **48**, 170–180 (2010).
311. Olad, A. li, Behboudi, S. & Entezami, A. li A. Preparation, characterization and photocatalytic activity of TiO2/polyaniline core-shell nanocomposite. *Bull. Mater. Sci.* **35**, 801–809 (2012).
312. Gilja, V. *et al.* Stability and synergistic effect of polyaniline/TiO2 photocatalysts in degradation of azo dye in wastewater. *Nanomaterials* **7**, 412 (2017).
313. Zhao, J., Wu, W., Sun, J. & Guo, S. Triplet photosensitizers: from molecular design to applications. *Chem. Soc. Rev.* **42**, 5323–5351 (2013).
314. Zhao, J. *et al.* Transition metal complexes with strong absorption of visible light and long-lived triplet excited states: from molecular design to applications. *RSC Adv.* **2**, 1712–1728 (2012).
315. Goldsmith, J. I., Hudson, W. R., Lowry, M. S., Anderson, T. H. & Bernhard, S. Discovery and High-Throughput Screening of Heteroleptic Iridium Complexes for Photoinduced Hydrogen Production. *J. Am. Chem. Soc.* **127**, 7502–7510 (2005).
316. Schäferling, M. The Art of Fluorescence Imaging with Chemical Sensors. *Angew. Chemie Int. Ed.* **51**, 3532–3554 (2012).
317. Fischer, L. H. *et al.* Referenced Dual Pressure- and Temperature-Sensitive Paint for Digital Color Camera Read Out. *Chem. – A Eur. J.* **18**, 15706–15713 (2012).
318. Tucker, J. W. & Stephenson, C. R. J. Shining Light on Photoredox Catalysis: Theory and Synthetic Applications. *J. Org. Chem.* **77**, 1617–1622 (2012).
319. Zou, Y.-Q. *et al.* Highly Efficient Aerobic Oxidative Hydroxylation of Arylboronic Acids: Photoredox Catalysis Using Visible Light. *Angew. Chemie Int. Ed.* **51**, 784–788

(2012).
320. Manangan, T., Shawaphun, S. & Wacharawichanant, S. Acetophenone and Benzophenone Derivatives as Catalysts in Photodegradation of PE and PP Films. in *Functionalized and Sensing Materials* vol. 93 284–287 (Trans Tech Publications Ltd, 2010).
321. Yousif, E., Salimon, J. & Salih, N. New stabilizers for polystyrene based on 2-N-salicylidene-5-(substituted)-1,3,4-thiadiazole compounds. *J. Saudi Chem. Soc.* **16**, 299–306 (2012).
322. Pinto, L. F. A., Goi, B. E., Schmitt, C. C. & Neumann, M. G. Photodegradation of polystyrene films containing UV-visible sensitizers. *J. Res. Updat. Polym. Sci.* **2**, 39–47 (2013).
323. Ong, C. B., Ng, L. Y. & Mohammad, A. W. A review of ZnO nanoparticles as solar photocatalysts: Synthesis, mechanisms and applications. *Renew. Sustain. Energy Rev.* **81**, 536–551 (2018).
324. Sharma, B. K., Gupta, A. K., Khare, N., Dhawan, S. K. & Gupta, H. C. Synthesis and characterization of polyaniline – ZnO composite and its dielectric behavior. **159**, 391–395 (2009).
325. Ameen, S., Akhtar, M. S. & Kim, Y. S. An effective nanocomposite of polyaniline and ZnO : preparation , characterizations , and its photocatalytic activity. *Colloid Polym Sci* **289**, 415–421 (2011).
326. Daikh, S., Zeggai, F. Z., Bellil, A. & Benyoucef, A. Chemical polymerization, characterization and electrochemical studies of PANI/ZnO doped with hydrochloric acid and/or zinc chloride: Differences between the synthesized nanocomposites. *J. Phys. Chem. Solids* **121**, 78–84 (2018).
327. Khan, A. A. & Khalid, M. Synthesis of Nano-Sized ZnO and Polyaniline-Zinc Oxide Composite : Characterization , Stability in Terms of DC Electrical Conductivity Retention and Application in Ammonia Vapor Detection. (2010) doi:10.1002/app.
328. Patil, S. L. *et al.* Structural, Morphological, Optical, and Electrical Properties of PANi-ZnO Nanocomposites. *Int. J. Polym. Mater. Polym. Biomater.* **61**, 809–820 (2012).
329. Gilja, V., Vrban, I., Mandić, V., Žic, M. & Hrnjak-Murgić, Z. Preparation of a PANI/ZnO composite for efficient photocatalytic degradation of acid blue. *Polymers (Basel).* **10**, 940 (2018).
330. Kumar, S. G. & Rao, K. S. R. K. Comparison of modification strategies towards enhanced charge carrier separation and photocatalytic degradation activity of metal oxide semiconductors (TiO2, WO3 and ZnO). *Appl. Surf. Sci.* **31517**–**3**, S0169-4332 (2016).
331. Chen, C. *et al.* Effect of Transition Metal Ions on the TiO2-Assisted Photodegradation of Dyes under Visible Irradiation: A Probe for the Interfacial Electron Transfer Process and Reaction Mechanism. *J. Phys. Chem. B* **106**, 318–324 (2002).
332. Sun, Q. & Xu, Y. Sensitization of TiO2 with Aluminum Phthalocyanine: Factors Influencing the Efficiency for Chlorophenol Degradation in Water under Visible Light. *J. Phys. Chem. C* **113**, 12387–12394 (2009).
333. Olad, A. & Nosrati, R. Preparation, characterization, and photocatalytic activity of polyaniline/ZnO nanocomposite. *Res Chem Intermed* **38**, 323–336 (2012).
334. Girish Kumar, S. & Koteswara Rao, K. S. R. Tungsten-based nanomaterials (WO3 & Bi2WO6): Modifications related to charge carrier transfer mechanisms and photocatalytic applications. *Appl. Surf. Sci.* **355**, 939–958 (2015).
335. Rajbongshi, B. M. & Samdarshi, S. K. Cobalt-doped zincblende–wurtzite mixed-phase ZnO photocatalyst nanoparticles with high activity in visible spectrum. *Appl. Catal. B Environ.* **144**, 435–441 (2014).
336. Denisyuk, I. Y., Pozdnyakova, S. A., Koryakina, I. G., Uspenskaya, M. V & Volkova, K. V. Polymer photodegradation initiated by ZnO nanoparticles. *Opt. Spectrosc.* **121**, 778–781 (2016).
337. Suryavanshi, R. D. *et al.* Nanocrystalline immobilised ZnO photocatalyst for

degradation of benzoic acid and methyl blue dye. *Mater. Res. Bull.* **101**, 324–333 (2018).
338. Zhang, Q. *et al.* Oxygen vacancy-mediated ZnO nanoparticle photocatalyst for degradation of methylene blue. *Appl. Sci.* **8**, 353 (2018).
339. Ngaloy, R. T. *et al.* Highly Efficient Photocatalysis by Zinc Oxide-Reduced Graphene Oxide (ZnO-rGO) Composite Synthesized via One-Pot Room-Temperature Chemical Deposition Method. *J. Nanotechnol.* **2019**, 1895043 (2019).
340. Asgari, E. *et al.* The comparison of ZnO/polyaniline nanocomposite under UV and visible radiations for decomposition of metronidazole: Degradation rate, mechanism and mineralization. *Process Saf. Environ. Prot.* **128**, 65–76 (2019).
341. Qi, K. *et al.* Transition metal doped ZnO nanoparticles with enhanced photocatalytic and antibacterial performances: Experimental and DFT studies. *Ceram. Int.* **46**, 1494–1502 (2020).
342. Ismael, M. The photocatalytic performance of the ZnO/g-C3N4 composite photocatalyst toward degradation of organic pollutants and its inactivity toward hydrogen evolution: The influence of light irradiation and charge transfer. *Chem. Phys. Lett.* **739**, 136992 (2020).
343. Neelgund, G. M. & Oki, A. ZnO conjugated graphene: An efficient sunlight driven photocatalyst for degradation of organic dyes. *Mater. Res. Bull.* **129**, 110911 (2020).